POLSKA AKADEMIA NAUK
KOMITET FIZYKI

ACTA PHYSICA POLONICA

DWUMIESIĘCZNIK

Vol. XIV — Fasc. 5

WARSZAWA 1955

First reprint by PWN — Polish Scientific Publishers 1969

ZUR FRAGE DER ADDITIVITÄT DER PARACHORE VON LÖSUNGEN

Von Marian Puchalik

Physikalisches Institut der Schlesischen L. Waryński Medizinischen Akademie, Rokitnica

(Eingegangen am 10. Januar 1955)

In der vorliegenden Arbeit wurde die Abhängigkeit der Parachore der Lösungen von ihrer Konzentration untersucht. Die Resultate der Messungen zeigen, dass die Additivität der Parachore der Lösungen nur in verhältnismässig seltenen Fällen zutrifft. Es wurden zwei Gleichungen vorgeschlagen, die die funktionelle Abhängigkeit der Parachore der Lösungen von ihrer Konzentration ausdrücken. Bemerkenswert ist die Abnahme der Parachore der stark verdünnten Lösungen mit wachsender Konzentration im Fällen, in denen das Parachor der gelösten Substanz das des Lösungsmittels weit übertrifft.

Das Problem der Additivität der Parachore von Lösungen ist sowohl vom Standpunkt der Theorie wie auch von dem der messtechnischen Praxis wichtig. Die Feststellung der funktionellen Abhängigkeit der Parachore der Lösungen von der Konzentration kann den Ausgangspunkt für die theoretische Deutung der Erscheinungen auf der freien Oberfläche der Lösungen bilden. Anderseits ist dieses Problem eng mit den Bestrebungen verschiedener Forscher gebunden, das Parachor der gelösten Substanz aus den Messungen an Lösungen und an den Lösungsmitteln zu berechnen.

Das Parachor der Lösungen wird bekanntlich durch folgende Formel definiert

$$P_{12} = (M_1 f_1 + M_2 f_2) \frac{\sigma_{12}^{1/4}}{\varrho_{12}} \tag{1}$$

(P_{12} bezeichnet das Parachor der Lösung, σ_{12} und ϱ_{12} die Oberflächenspannung, bzw. die Dichte der Lösung, M_1 und M_2 die Molgewichte, f_1 und f_2 die Molbrüche des Lösungsmittels und des gelösten Stoffes).

Zur Berechnung des Parachors der gelösten Substanz bedient man sich der Formel von Hammick und Andrew (1929) oder der Formel von Skramowsky (1944, nach Soucek 1945). Die erste dieser Formel setzt die Additivität des Parachors der Lösungen voraus:

$$P_{12} = P_1 (1 - f_2) + P_2 f_2, \tag{2}$$

(P_1 und P_2 sind die Parachore des Lösungsmittels und der gelössten Substanz).

Nach Skramovsky wird das Parachor der gelösten Substanz aus der folgenden Gleichung berechnet:

$$P_2 = M_2 \frac{\left(\frac{\Delta\sigma}{f_2} + \sigma_1\right)^{1/4}}{\frac{\Delta\sigma}{f_2} + \varrho_1} \tag{3}$$

($\Delta\sigma$ ist die Differenz der Oberflächenspannungen der Lösung und der gelösten Substanz, $\Delta\varrho$ die entsprechende Differenz der Dichten). In der Formel von Skramovsky wird es angenomen, dass die Oberflächenspannung der Lösung der folgenden Gleichung genügt:

$$\sigma_{12} = \sigma_1 (1 - f_2) + \sigma_2 f_2 \tag{4}$$

Nach den Beobachtungen des Verfassers (Puchalik 1954) treffen diese beiden Voraussetzungen oft nicht zu. Deswegen stellte sich der Verfasser die Aufgabe die funktionelle Abhängigkeit der Parachore der Lösungen von der Konzentration dieser Lösungen näher zu untersuchen, mit der Absicht die Grundlagen für die Berechnung der Parachore der gelösten Substanzen auch für solche Fälle zu schaffen, in denen die Additivität nicht mehr zutrifft.

Das Untersuchungsmaterial

Zur Lösung des oben angedeuteten Problems bediente sich der Verfasser der Resultate seiner vorigen Arbeit (Puchalik 1954) sowie der Messungen von Harkins und Grafton (1921). Ausserden wurde speziell für diesen Zweck die Oberflächenspannung der Lösungen der α — und β — Naphthole in Aethylaether und in Aethylalkohol gemessen. Die genannten Substanzen wurden nach den in früheren Arbeiten des Verfasser angewandten Methoden gereinigt (Puchalik 1932, 1954).

Die Untersuchungsmethode

Zur Messung der Oberflächenspannung wurde die Methode des maximalen Luftdrucks in Blasen von Cantor-Rehbinder (Rehbinder 1935) angewandt. Als Kapillaren wurden bakteriologischen Mikropipetten benutzt, welche sich zu diesem Zwecke als gut geeignet erwiesen haben. Als Manometerflüssigkeit wurde raffiniertes Petroleum angewandt. Die Änderung des Luftdruckes erfolgte langsam genug, damit man nach einiger Übung die Meniskushöhe im Moment des Abreissens der Luftblase vermittels des Komparators leicht ablesen könne. Die Genauigkeit der Messung δ betrug c. 0,3%. Kontrollmessungen gaben gut übereinstimmende Werte mit denen die mittels der Steighöhenmethode erhalten wurden. Im Vergleich zur der Steighöhenmethode ist die benutzte Rehbindersche Methode genauer, da die Resultate ihrer Anwendung

nicht so stark durch die Beschaffenheit der Wände der Kapillaren beeinflusst werden.

Die Konstanthaltung der Temperatur wurde durch ein Thermostat nach Höppler gesichert.

Besprechung der Resultate

Die Resultate der Messungen sind in den Tabellen 1 — 8 und in den Diagrammen 1 — 3 zusammengestellt. Aus den gewonnenen Resultaten geht deutlich hervor, dass die Additivität der Parachore von Lösungen nur in einigen der untersuchten Fällen zutrifft. Die untersuchten Lösungen kann man in 3 Gruppen einteilen. Zur ersten Gruppe gehören die Lösungen von Aethylaether in Benzol und von Nitrobenzol in Benzol. Wie aus den Tabellen 1 und 2 ersichtlich ist, kann man die funktionelle Abhängigkeit des P_{12} von f_2 in diesem Falle durch die vom Verfasser vorgeschlagene Formel

$$P_{12} = P_1 (1 - f_2) + P_2 f_2^K \tag{5}$$

ausdrücken. Wenn man nämlich aus irgend einer Konzentration der betreffenden Lösungen unter Zugrundelegung der von unmittelbaren Messungen stammenden Werte für P_2 den Exponenten k berechnet, so bekommt man für die anderen Konzentrationen solche Werte von P_2, die mit den unmittelbar gemessenen innerhalb der Fehlergrenzen gut übereinstimmen. Damit scheint die Formel (5) für diese Lösungen berechtigt zu sein.

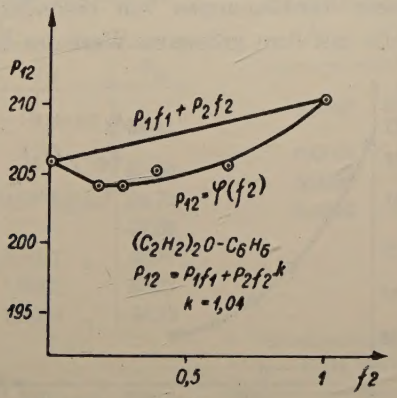

Fig. 1

Anders liegen die Verhältnisse für die zweite Gruppe von Lösungen. Zu dieser Gruppe gehören die Lösungen von Aethylalkohol in Wasser (Puchalik 1954) und von β — Naphthol in Aethylalkohol. In dieser Gruppe nimmt P_{12} mit wachsender Konzentrationen anfangs ab, obwohl die Parachore der gelösten Substanzen die des Lösungsmittels weit übertreffen. Von einer bestimmten Konzentration ab, steigt P_{12} linear mit wachsenden f_2 und bei $f_2 = 1$ erreicht den Wert P_2 für die reine gelöste

Substanz (Tab. 7 und Fig. 2). In diesem Falle kann man im Bereiche der nicht allzu kleinen Konzentrationen die $P_{12} = \varphi(f_2)$ – Kurve durch die folgende, ebenfals vom Verfasser vorgeschlagene, Gleichung ausdrücken

$$P_{12} = K_0 P_1 (1 - f_2) + P_2 f_2 \tag{6}$$

wo K_0 einen echten, konstanten Bruch darstellt.

Die Parachore der Lösungen von Aethylalkohol in Benzol (Puchalik 1954) und von α – Naphthol und β – Naphthol in Aethylaether bilden additive Funktionen der

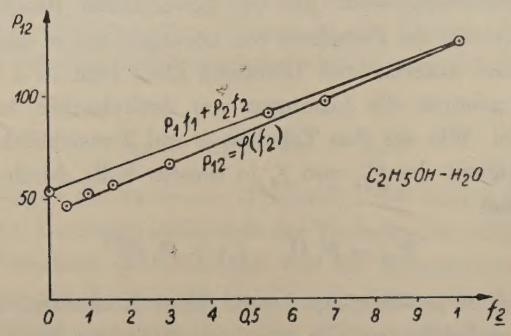

Fig. 2

Konzentrationen, Tab. 4 und 5. Diese Additivität der Parachore kann man als einen Grenzfall der oben besprochenen Fälle für $k=1$ und $k_0=1$ betrachten. Im Fällen wo die Additivität nicht zutrifft ist die Abnahme des Parachors mit wachsender Konzentration im Bereiche grosser Verdünnungen von besonderem Interesse, obwohl als gelöste-Substanz immer die mit dem grösseren Wert des Parachors gewählt wurde.

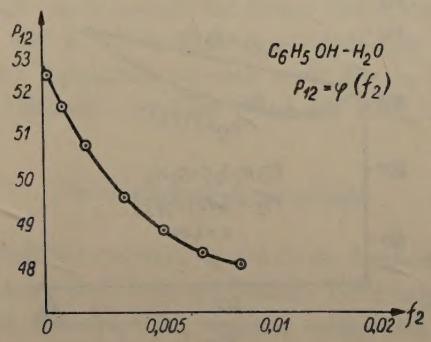

Fig. 3

Ein vortrefliches Beispiel dieses merkwürdigen Verhaltens der Parachore von stark verdünnten Lösungen bilden die wässrigen Lösungen von Phenol. In Tab. 3 und Fig. 3 sind die Werte der Parachore dieser Lösungen bei verschiedenen Konzentrationen zusamengestellt. Diese Werte wurden aus sehr genauen Bestimmungen der Oberflächenspannung von Harkins und Grafton (1921) berechnet.

Tab. 1.

$(C_2H_5)_2O - C_6H_6$ $t = 20°C \pm 0{,}1°C$
$K = 1{,}042$

f_2	P_{12}	P_2
0,0000	206,0	
0,1649	204,1	210,8
0,2566	204,3	211
0,3948	205,3	212
0,6379	206,0	210
1,0000	210,8	210,8

Tab. 2.

$C_6H_5NO_2 - C_6H_6$ $t = 20°C \pm 0{,}1°C$
$K = 1{,}093$

f_2	P_{12}	P_2
0,0000	206,0	
0,1821	210,3	262,0
0,2545	217,9	269
0,3935	222,5	263
0,6074	232,6	254
0,7603	246,6	260
1,0000	262,0	262,0

Tab. 3.

$C_6H_5OH - H_2O$ nach Harkins und Grafton
$t = 20°C$

f_2	σ_{12}	d_{12}	P_{12}
0,00018	71,69 Dynen/cm		52,41
0,00090	66,50 „		51,60
0,00181	61,12 „	0,9978 g/cm³	50,72
0,00366	53,97 „		49,63
0,00541	49,13 „	0,9987 „	48,77
0,00715	45,84 „	1,0002 „	48,27
0,00892	44,02 „	1,0009 „	48,12

Tab. 4.

$\alpha - C_{10}H_7OH - (C_2H_5)_2O$ $t = 20°C \pm 0{,}1°C$
$P_1 = 209{,}3$

f_2	σ_{12}	P_{12}	P_2
0,0248	16,95 Dynen/cm	213,6	320
0,0626	18,50 „	221,6	333
0,1083	19,27 „	226,4	366
0,1398	20,65 „	234,4	342

Tab. 5.

$\beta - C_{10}H_7OH - (C_2H_5)_2O$ $t = 20°C \pm 0{,}1°C$
$P_1 = 209{,}3$

f_2	σ_{12}	P_{12}	P_2
0,0602	17,73 Dynen/cm	216,0	322
0,0936	19,30 „	223,0	360
0,1070	20,04 „	223,6	344
0,1277	20,35 „	226,7	345

Tab. 6.

$\alpha - C_{10}H_7OH - C_2H_5OH$ $t = 20°C \pm 0{,}1°C$
$P_1 = 126{,}9$

f_2	σ_{12}	P_{12}
0,0056	22,3 Dynen/cm	127,5
0,0112	22,3 „	127,4
0,0230	22,3 „	129,5
0,0601	22,2 „	138,0

Tab. 7.

$\beta - C_{10}H_7OH - C_2H_5OH$ $t = 20°C \pm 0{,}1°C$

f_2	σ_{12}	P_{12}
0,0052	20,04 Dynen/cm	122,7
0,0180	18,51 „	123,9
0,0262	18,19 „	125,5
0,0394	18,03 „	127,6

Tab. 8.

$t = 20°C \pm 0{,}1°C$

$\alpha - C_{10}H_7OH - C_6H_6$		$\beta - C_{10}H_7OH - C_6H_6$	
f_2	σ_{12}	f_2	σ_{12}
0,0395	27,0 Dynen/cm	0,0276	28,4 Dynen/cm
$\alpha - C_{10}H_7OH - H_2O$		$\beta - C_{10}H_7OH - H_2O$	
f_2	σ_{12}	f_2	σ_{12}
0,0007	60,3 Dynen/cm	0,00005	62,9 Dynen/cm

Leider kann man wegen der schweren Löslichkeit des Phenols in Wasser in diesem Falle den Gang der $P_{12} = \varphi(f_2)$ – Kurve auch für grössere Konzentrationen nicht bestimmen.

Dasselbe betrifft die Lösungen der α — und β – Naphthole in Wasser und in Benzol.

Da aber die Werte der Parachore verschiedener Lösungen im Bereiche sehr kleiner Konzentrationen im Allgemeinen nicht bestimmt sind und sie genügen auch nicht den Formeln für grössere Konzentrationen, wird vom Verfasser das Problem der genaueren Untersuchung solcher Lösungen wie auch das der theoretischen Deutung dieser Erscheinungen gestellt. Bezugnehmend auf die in Tab. 6 dargestellten Ergebnisse, muss die Sonderstellung der Parachorwerte der Lösung von α – Napthol in Aethylalkohol näher besprochen werden. In diesem Falle bildet das Parachor der Lösung keine streng additive Funktion der Konzentrationen, es nimmt aber monoton mit wachsender Konzentration zu. Bemerkenswert ist, dass die Oberflächenspannung in diesem Falle innerhalb der Fehlergrenzen als konstant anzusehen ist.

Die zur Untersuchung nötigen α – und β – Naphthole wurden dem Verfasser durch das Institut für Physiologische Chemie der Schlesischen Medizinischen Akademie geliefert. Dem Leiter dieses Instituts, Herrn Prof. Dr Stanislaus Jóźkiewicz, spricht der Verfasser seinen verbindlichsten Dank aus.

КРАТКОЕ СОДЕРЖАНИЕ

Пухалик, К ВОПРОСУ ОБ АДДИВИТЕТЕ ПАРАХОРОВ РАСТВОРОВ.

В настоящей работе исследована зависимость парахоров растворов от их концентрации. Результаты измерений указывают на то, что аддивитивность парахоров растворов сравнительно редко случается. Были предложены два уравнения, которые выражают функциональную зависимость парахоров растворов от их концентрации. Замечательное уменьшение парахоров сильно разбавленных растворов с возростающей концентрацией в случаях, в которых парохор разбалвенного вещества много превышает парахор растворителя.

LITERATURHINWEISE

Hammick, D. L. und Andrew, L. W., *J. chem. Soc.*, **55**, 756 (1929).

Harkins, W. D. und Grafton, E. H. *J. chem. Soc.*, **47**, 330 (1921).

Puchalik, M., *Acta phys. Polon.*, **13**, 159 (1954).

Puchalik, M., *Bull. internat. Acad. Polon. Sci.*, 22 (1932).

Rehbinder, *Kapitel über Oberflächenspannug in Naumow's Lehrbuch der Kolloidchemie*, Moskau 1935.

Soucek, B., *Čas. Česk. Lek.* **58**, 57 (1945).

AN INTEGRATING APPARATUS FOR THE SCHRÖDINGER EQUATION. II

By K. Antonowicz

Department of Physics, Nicholas Copernicus University, Toruń

(Received February 17, 1955)

Several improvements have been introduced in the integrating apparatus for the Schrödinger equation, (Antonowicz 1953). The apparatus was calibrated by means of the Morse potential and its harmonic approximation. For verification purposes eigenvalues were determined for the harmonic oscillator and the Morse potential. The eigenvalues obtained by means of the apparatus agree within 1 per cent with the theoretical values. One of the eigenfunctions for Morse's potential was compared with a theoretical curve. A very good agreement between them was found.

I. Introduction. In an earlier paper (Antonowicz 1953) a description of an integrating apparatus for the Schrödinger equation was given. The apparatus is based on the analogy between the Schrödinger equation and that of the motion of a magnetic needle in a homogeneous magnetic field, i.e. on the analogy between the equations

$$\frac{d^2\psi}{dx^2} + \frac{2\mu}{\hbar^2}[E - U(x)]\,\psi = 0 \tag{1}$$

$$\frac{d^2 a}{dt^2} + \frac{m}{B}[H_0 - H(t)]\,a = 0 \tag{2}$$

After our first paper appeared, we had the possibility of becoming acquainted with a paper of Bullard and Moon (1931), from which we learned that the principle on which the construction of our apparatus was based was similar that already used by these authors. However, the realization of the principle was different. Apart from technicalities (e.g. the use of a movable needle instead of a movable coil) there were differences resulting from the desire of eliminating as much as possible the share of the experimenter in the process of solving the equation.

By means of the described apparatus we were able to obtain eigenfunctions (of the harmonic oscillator) with a very great accuracy. We met, however, with serious difficulties in determining the eigenvalues and calibrating the apparatus. The stability was too bad and the sensitivity for external disturbances too great to enable accurate

measurements to be made. Thus necessary steps were taken to improve the stability and precision of the apparatus; namely

(1) by application of an astatic needle system;

(2) by stabilizing the D. C. amplifier and the speed of motor rotations;

(3) by construction of an apparatus for obtaining accurate „potential curves".

A short description of the technical improvements, the method of calibrating the apparatus, as well as the results obtained by integrating the Schrödinger equation for Morse's potential are given below.

II. The magnetic needle. The oscillations of a magnetic needle suspended on a cocon fibre are strongly damped if the amplitudes are rather great, whereas at small amplitudes external disturbances cause continual oscillations of the needle. The external disturbances are of two kinds: mechanical and magnetic. The mechanical disturbances might be eliminated by a shock-proof suspension system. It is better, however, to eliminate them by using a moving system with such a high moment of inertia that the system becomes insensitive to these external mechanical disturbances; an additional advantage of such a system is that the damping of oscillations becomes comparatively small and the analogy between equations (1) and (2) closer. In our apparatus the moment of inertia of the astatic needle system has been increased by means of a lead cylinder (external diameter 16 mm, inner diameter 6 mm and 5 mm in height).

Magnetic disturbances are eliminated by using an astatic needle system, the needles being suspended one above the other at a distance of 10 cm. The needles of $2\times2\times8$ mm were made of magnetic steel. Each needle is in the homogeneous part of the magnetic field given by two Helmholtz systems of coils. Each of the Helmholtz systems has 3 independent windings. The rôle of the first winding is to give $H(t)$, the second and the third ones are used for precise adjustment of H_0 for finding the eigenvalues. We are unable to measure currents by means of our milliammeters with an exceeding precision 1 per cent.; thus it is very difficult to adjust the currents with a better precision. In searching for the eigenvalues, however, it is necessary to regulate the intensity of the field with a precision of at least 0,01 per cent. This difficulty is solved by the use of two windings. One of them with a great number of turns is situated near the needle, the other one having but a few turns is placed at the farthest end of the coils. The same current in the first winding produces a considerably stronger field than it would produce flowing in the second one. Searching for the eigenvalues, we first regulate the intensity of the current in the first winding, with as much precision as the milliammeter permits, and then in the second one, which produces small changes in the magnetic field even if changes of the current are considerable. In this way a subtle regulation of the magnetic field is achieved. The measuring of the magnetic field is carried out independently of the measuring of the current (see below).

III. The time-dependent magnetic field. The field $H(t)$ is produced by the amplified current of a photocell. The intensity of light falling on the photocell is regulated by a disc („potential curve") revolving at constant speed, the edge of which is cut in

the form of the $U(x)$ function in the polar system. To make sure that all the discs are made on the same scale and with the greatest precision possible, a special apparatus has been constructed, (see Fig. 2).

It consists of an iron plate, 50 cm in diameter, that may be turned round axis O with an angular scale at the edge divided into 0,5°. Above the plate a micrometer

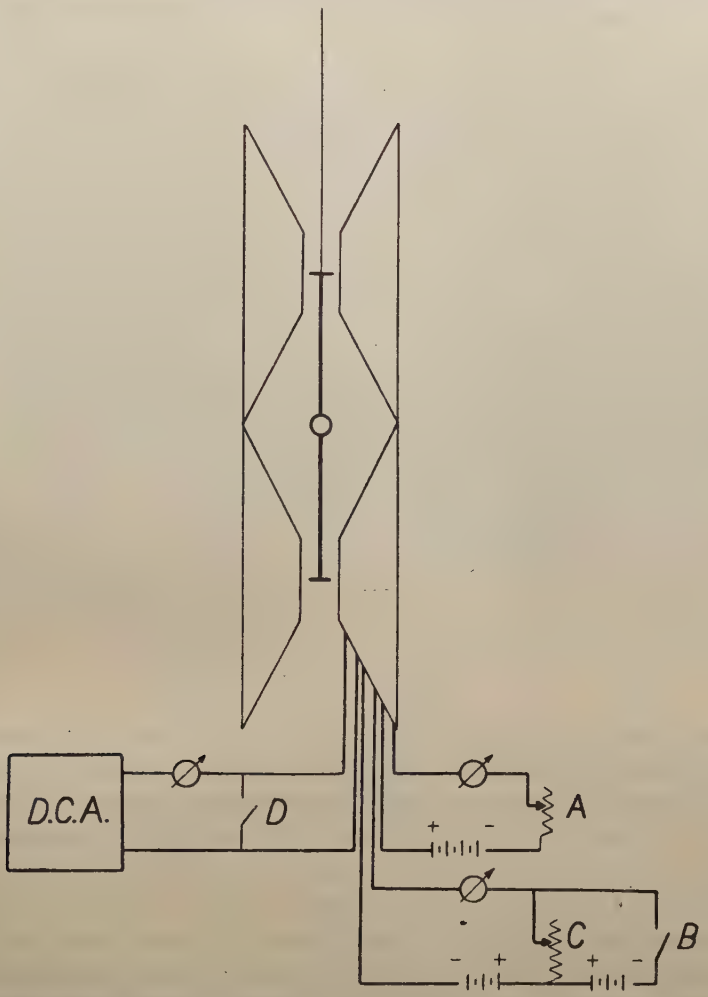

Fig. 1. Astatic needle system. DCA — direct current amplifier. A — resistor for coarse regulating of H_0. C — resistor for fine regulation of H_0. B — switch used to stop the needle. D — switch used to switch off $H(t)$

screw is fastened which permits to shift slide B by means of knob C along the radius of the plate; the position of the slider can be read with a precision not worse than 0,01 mm. The slider is provided with a puncher. When puncher B is pressed it makes a small trace (hole) on the paper placed on the plate. The equation of the curve being known,

the calculated points may be very accurately put down on paper and thus enable a very accurate „potential curve" to be cut out.

The direct current amplifier must be characterized by an exact reproduction of currents and, apart from this, by a great stability and considerable current output. In order to ensure stability of the amplifier its power sources have been stabilized. The incandescent tubes were fed by a battery of accumulators. The plate voltage were fed

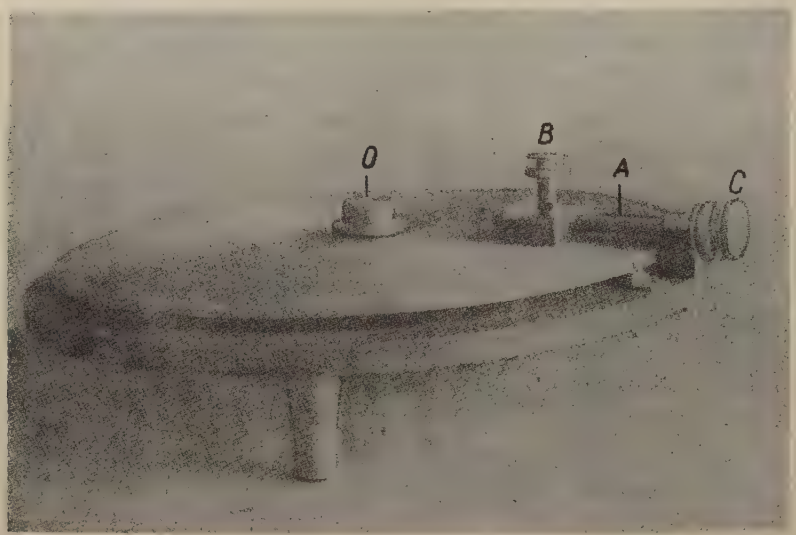

Fig. 2. The apparatus for marking the potential curve. O — axis of the plate. A — micrometer screw. B — puncher. C — knob of the screw

by a rectifier stabilized by a tubes system which, in turn, was fed by mains through a magnetic stabilizer. Our amplifying system is generally known as a „bridge circuit". A certain shifting of the working point is observed which, however, does not affect the precision of measurements, since a suitable correction in the eigenvalue can be easily made.

The stability of the speed of the motor plays an important rôle. A small converter fed by direct current from a battery of accumulators is used as motor. The dynamo of the converter feeds a stabilivolt. As it is known, small voltage changes produce great current changes in the stabilivolt. Thus the load of the converter is changing and regulates the motor speed. The speed is checked by means of a milliammeter introduced into the converter circuit. *A* 0,01 per cent. change in speed causes c. 1 mA change of the current. A resistance on the side of motor feeding permits to regulate the motor speed up to the required value.

IV. The eigenvalues. The value of the constant magnetic field H_0 by which the function satisfies the boundary conditions, determines the eigenvalue. H_0 is not directly proportional to the eigenvalue; it must be corrected by subtracting the field value

due to the constant component of the amplifier current, the turning moment of the cocon fibre, as well as by the value of the earth magnetic field with which the movable system interacts in spite of the astaticity of the needle system. Thus a certain value H_{00} must be subtracted from H_0 in order to obtain a value proportional to the eigenvalue E_n. The value H_{00} is easy to determine in the case of the harmonic oscillator, in which case the difference between the energy levels is constant and equal to $h\nu$, the lowest level having the value $h\nu/2$. Thus subtracting from the lowest measured eigenvalue the value corresponding to $h\nu/2$ yields H_{00}. The value H_{00} is then subtracted also from all the other eigenvalues measured.

The magnetic field corresponding to the eigenvalue is determined in the following way: we let the needle oscillate in the field H_0; in this case the curve obtained by means of the apparatus is a sine curve, from which we calculate H_0. Table I contains the eigenvalues thus determined for the harmonic oscillator in the units $h\nu = 1$.

Table I. *Eigenvalues of the harmonic oscillator obtained by means of the apparatus*

Quantum number	Measured	Should be	Error
0	0,5	0,500	—
1	1,493	1,500	0,5 per cent
2	2,520	2,500	0,8 „ „
3	3,509	3,500	0,3 „ „
4	4,526	4,500	0,6 „ „
5	5,508	5,550	0,1 „ „
6	6,510	6,500	0,2 „ „
7	7,490	7,500	0,1 „ „
8	8,493	8,500	0,1 „ „

V. Calibration of the apparatus. In order to calibrate the apparatus eigenfunctions and eigenvalues have been found for the Morse potential (Morse 1929) as well as for its harmonic approximation. As it is known this potential has the form

$$U(r) = D(1 - e^{-\beta(r-r_0)})^2$$

and the frequancy of small classical oscilations about the point r_0 is

$$\nu_0 = \frac{a}{2\pi}\left(\frac{2D}{\mu}\right)^{1/2}$$

Therefore, if we take then constant factor in the expression for the potential energy of the harmonic oscillator as equal to

$$2\pi^2\nu_0^2\mu = a^2D,$$

such a harmonic oscillator will represent the zero approximation to the Morse potential.

We assume the following values of the parameters:

$$D = 50\,000 \text{ cm}^{-1}$$
$$a = 1{,}7 \text{ A. U.}$$
$$r_0 = 1{,}3 \text{ A. U.}$$

The potential curves were made by means of the special apparatus described above (Fig. 2) in the scale $1° = 0{,}01$A. U., and 1 mm $= 1{,}10^{-3}$ cm^{-1} $= 9{,}9275 \cdot 10^{-9}$ erg. The eigenvalues obtained for the potential curves were in arbitrary units. Since the difference between the eigenvalues of the harmonic oscillator is equal to $h\nu_0$, and the distribution of the eigenvalues for Morse's potential is given by

$$E_n = -D + h\nu_0 \left(n + \frac{1}{2}\right) - \frac{h^2 \nu_0^2}{4D} \left(n + \frac{1}{2}\right)^2,$$

E_n and $h\nu_0$ being given in arbitrary units, it was possible to determine immediately $h^2\nu_0^2/4D$ in the same units. The absolute values of $h\nu_0$ and $h^2\nu_0^2/4D$ may be also determined in absolute units for a reduced mass μ, which results from the ratio of the magnetic moment of the needle m to its moment of inertia B, i. e. from m/B (*Eq.* (2)). Thus it is possible to solve the problem for a certain mass μ which may be determined from the above data. We have obtained by means of the apparatus:

$h\nu_0 = 1129$ in arbitrary units
$h^2\nu_0^2/4D = 20{,}7$ in the same units. The ratio of these values does not depend on the units and is equal to 54, 541.

Exact solutions of the Schrödinger equation for the Morse potential are.

$$h\nu_0 = h \left(\frac{a^2 D}{2\pi^2 \mu}\right)^{1/2}$$

$$\frac{h^2 \nu_0^2}{4D} = \frac{h^2 a^2}{8\pi^2 \mu}$$

Hence

$$\left(\frac{h\nu_0}{\frac{h^2 \nu_0^2}{4D}}\right)^2 = \frac{32\pi^2 \mu D}{h^2 a^2} = 54{,}541^2$$

and after substituting the assumed parameter values and the values of universal constants, we obtain $\mu = 1{,}20\,10^{-24}\,g$.

It is obvious that, the mass corresponding to the ratio m/B being known, it is easy to adapt the apparatus to another mass by changing the value m/B (practically by changing the moment of inertia B). The same effect may be reached without changing this moment of inertia, either by changing the scale of the potential curve, or by changing the speed of disc rotations. Thus the apparatus can be adapted to the solution of problems with any mass.

Assuming the mass $\mu = 1{,}2\,10^{-24}g$, we can calculate all the quantities we are interested in and compare them with those given by the apparatus, namely

$h\nu_0$ — in arbitrary units, obtained by means of the apparatus = 1129;
$h\nu_0$ — calculated theoretically = $7{,}285\ 10^{-13}$ erg, theorefore the arbitrary energy unit = $6{,}4526\ 10^{-16}$ erg. We can now calculate the eigenvalues for the assumed Morse potential, e.g. in ergs, both from the data obtained by means of the apparatus and from Morse's expression for eigenvalues. The results are given in Table II.

Table. II. *Eigenvalues for Morses potential*

Quantum number	Eigenvalues obtained by means of the apparatus 10^{-13}	Eigenvalues calculated theoretically 10^{-13}	Difference between obtained and calculated eigenvalues
0	—95,728	—95,666	0,08 per cent
1	—88,400	—88,649	0,3 „ „
2	—81,950	—81,949	0,00 „ „
3	—75.655	—75,417	0,3 „ „
4	—69,405	—69,202	0,4 „ „
5	—63,324	—63,255	0,1 „ „
6	—57,906	—57,576	0,6 „ „
7	—51,751	—52,164	0,8 „ „

The absolute error is nearly the same for all eigenvalues, therefore the relative error for small eigenvalues is rather greater; the relative error in the differences between neighbouring energy levels reaches several per cent.

VI. Eigenfunctions for Morse's potential. In the previous paper (1953) eigenfunctions of the harmonic oscillator, obtained by means of the apparatus, were publ-

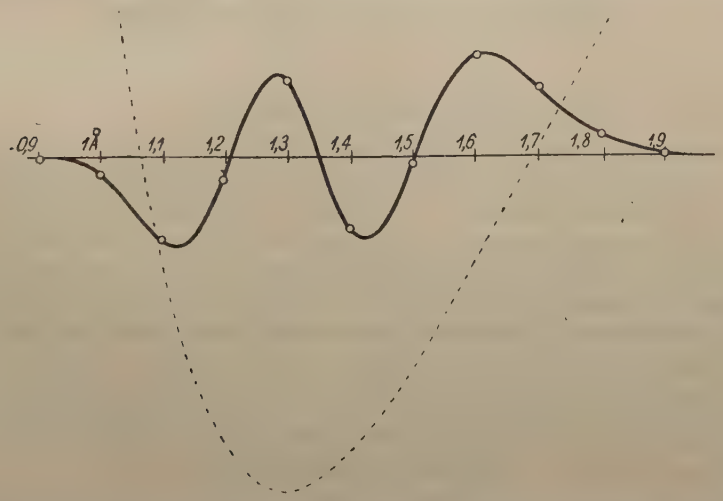

Fig. 3. Eigenfunction obtained by means of the apparatus. The points inside the circles mean theoretical points. The dotted line is the lower part of the (Morse's) potential curve

ished and showed very good agreement with the points calculated theoretically. However, the shape of the eigenfunctions of the harmonic oscillator does not depend on the specific values of the constants in the potential functions. It was therefore interesting to verify the accuracy of the eigenfunctions of Morse's potential, whose shape is

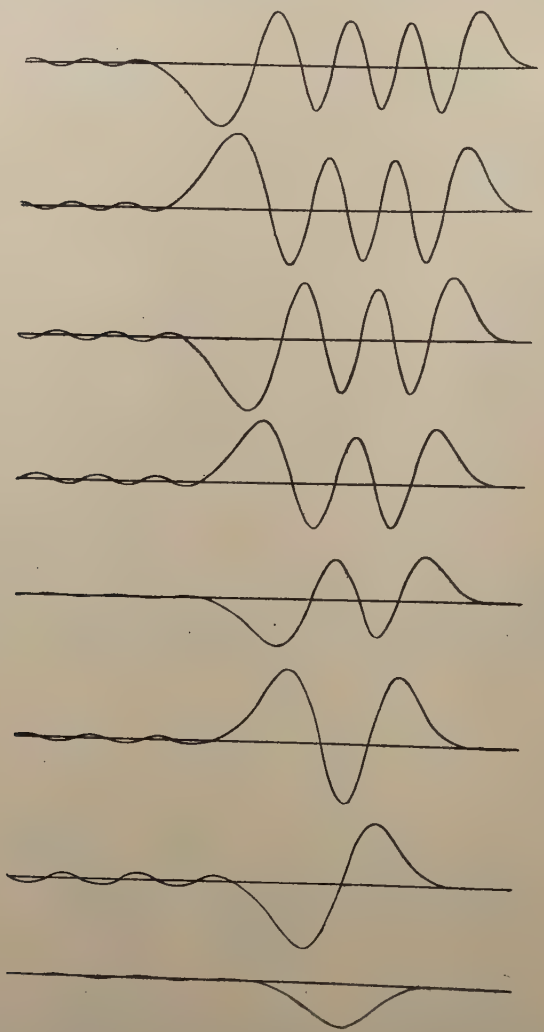

Fig. 4. 8 eigenfunctions of Morse's potential. All the curves are redrawn for reproduction purposes

determined by the constants. The eigenfunctions given by the apparatus are not normalized. Thus we are free to choose arbitrary one constant, e. g. the normalizationfactor. The radial eigenfunction for Morse's potential is given by the expression:

$$\psi = C \cdot e^{-de^{-a(r-r_0)}} [2de^{-a(r-r_0)}]^{\frac{K-2n-1}{2}} L_{K-n-1}^{K-2n-1} [2de^{-a(r-r_0)}],$$

where in the case in question

$$d = \frac{2\pi\sqrt{2\mu D}}{ah} = 27{,}1$$
$$a = 1{,}7$$
$$r_0 = 1{,}3$$
$$k = 2d = 54{,}2$$

For verification purposes an eigenfunction of three zeros was chosen, i. e. for $n = 3$. The dimensions of the curve obtained directly from the apparatus are too small to make accurate determination of its errors possible. Therefore the curve was magnified. The length of the magnified curve was 1 m and the maximum amplitude 0,15 m.

By substituting the values of the constants, we obtained the following expression for the eigenfunction

$$\psi = 1.10^{15}\, e^{-27{,}1\, e^{-1{,}7\,(r-1{,}3)}} \cdot [e^{-1{,}7\,(r-1{,}3)}]^{23{,}6} \cdot [15{,}922\, e^{-5{,}1\,(r-1{,}3)} - 44{,}241\, e^{-3{,}4\,(r-1{,}3)} + 40{,}159\, e^{-1{,}7\,(r-1{,}3)} - 11{,}9049] \text{ mm}$$

It is convenient to put

$$x = e^{-1{,}7\,(r-1{,}3)}$$

to get a simpler expression, namely

$$\psi = 1.10^{15}\, e^{-27{,}1x}\, x^{23{,}6}\, [15{,}922\, x^3 - 44{,}241\, x^2 + 40{,}1596\, x - 11{,}9049]$$

In spite of this simplification the calculation of the points of the curve is very tedious. Therefore the calculations were carried out only for $r = 0{,}9;\ 1{,}0;\ \ldots 1{,}9$ *A. U.* The teoretical points appeared to be situated within the breadth of the line (Fig. 3). The points inside the circles means theoretical points.

Fig. 4 shows 8 eigenfunctions of Morse's potential, from which the fourth was used for checking the exactitude of the apparatus.

The author expresses his gratidude to professor A. Jabłoński for helpful discussions and support throughout the work.

КРАТКОЕ СОДЕРЖАНИЕ

Антонович. ПРИБОР ДЛЯ ИНТЕГРИРОВАНИЯ УРАВНЕНИЯ ШРЕДИНГЕРА II.

Введено много улучшений в приборе для интегрирования уравнения Шредингера. Прибор был калиброван при помощи потенциала Морса и его гармонического приближения. Для проверки действия прибора были определены значения собственные для гармонического осциллятора и потенциала Морса. Значения собственные полученные при помощи прибора, согласуются с теоретическими значениями с точностью до 1%. Одна из функций для потенциала Морса была сопоставлена в теоретической кривой. Получена очень хорошая согласованность между обеими кривыми.

REFERENCES

Antonowicz, K., *Acta phys. Polon.*, **12**, 163 (1953).
Bullard, E. C. and Moon, P. B., *Proc. Cambridge Phil. Soc.*, **27**, 546 (1931).
Morse, P. M., *Phys. Rev.*, **34**, 57 (1929).

DEPENDENCE OF THE DIELECTRIC PROPERTIES OF CERAMIC $BaTiO_3$ FOR HIGH FREQUENCY CURRENTS ON THE TECHNOLOGY OF THE PREPARATION OF SAMPLES

By M. Jeżewski and T. Piech

Institute of Technical Physics, Mining Academy, Cracow

(Received April 4, 1955)

The dependence of the dielectric constant and the ceramic $BaTiO_3$ losses on the way of preparing samples has been investigated. The method of measurements of the dielectric constant of materials having very high dielectric constants has been worked out with the help of high frequency currents, as well as the method of measurements of losses. Four groups of $BaTiO_3$ samples, marked *A*, *B*, *C*, *D*, have been prepared, each of them being obtained from the previous one by means of thorough grinding, pressing, and resintering at a temperature of about 1350°C. The last group *D* remained particularly long in the oven: about 130 hours, including the time of heating and cooling. It has been proved that the dielectric constant of each successive group of samples is at all temperatures considerably higher than the dielectric constant of the previous group. The losses of samples in the row *A*, *B*, *C*, *D* decrease gradually but not very significantly.

Introduction

The examination of the dielectric properties of ferroelectrics of the $BaTiO_3$ type are usually carried out with ceramic materials, which can be formed according to the desired shape and size, which is particularly important in practical applications. The comparison of the results of investigations carried out with single crystals and ceramic bodies shows that materials having multicrystalline structure behave, in general, similarly to crystals (Merz 1949, Rżhanov 1949, Mason and Matthias, 1954). For instance the dependence of the dielectric constant of the multicrystalline $BaTiO_3$ on different parameters is the same as for single crystals, and the difference exists only in the absolute value of this constant. This is due to the fact that while examining the ceramic samples one measures only an average value of the constant of the crystallites, their axis directions being distributed at random without any privileged direction in space. Yet in reviewing the already comprehensive literature on this subject, it can be stated that the data of various authors concerning the dielectric properties of the ceramic $BaTiO_3$ in weak fields, rather considerably differ in values (Roberts 1949, Rżhanov 1949, von Hippel 1950, Pająk 1950, Kazarnovskij 1954), in spite

of the fact that the samples were prepared by similar methods and that the dielectric constant of this material has been found to be independent of the current frequency up to $f = 10^8$ Hz. (Powles 1948, von Hippel 1950, Piekara 1950). It seems that the cause of these divergencies can by no means be ascribed to the possibility of the samples, examined by various authors, being prepared from different initial materials, thus containing possibly some significant impurities. Although it is well known that materials having a high dielectric constant are sensitive to the presence of certain additions, yet there is little probability that the commercially pure components, used for the synthesis, might have contained impurities in amounts able to cause such considerable divergences. Investigations were also made (Graf 1951) proving that there exist only small differences between the properties of the samples obtained from the initial materials with a high degree of spectroscopically examined purity and those of the samples prepared from commercially pure materials.

It is, however, possible that the dielectric properties of the ceramic $BaTiO_3$ depend on the technique of preparation of the samples. The aim of the present paper is to ascertain wheter these properties depend on the way of preparing and the time of sintering the samples, and if they do, in what a manner. In order to find it out the dielectric constants and the dielectric losses of the ceramic samples prepared in various ways (described below) from the same initial materials have been measured at different temperatures. Measurements were made by means of a 5 MHz frequency current at temperatures ranging from room temperature up to temperatures considerably higher than the Curie point (of about 170°C).

Technology of preparing the ceramic samples

Barium carbonate ($BaTiO_3$) indicated as „chemically pure" as well as titanium oxide (TiO_2) were weighed in the molar ratio of 1 : 1 and mixed thoroughly by long grinding in a porcelain mortar. From this mixture tablets 14 mm in diameter and about 5 mm thick were formed under a pressure of 2400 kG/cm². The sintering of these tablets took place in an electric furnace of fire clay at a temperature of 1350°C. Heating up to this temperature lasted about 4 hours and for the same period of time the samples remained in the oven at peak temperature, while cooling lasted about 10 hours. According to data from literature (Trzebiatowski 1952, Wojciechowska and Damm 1952) in these conditions the synthesis of barium titanate should be completely accomplished. In order to avoid diffusion of foreign atoms from the liner, on which the samples were placed in the oven during the sintering, a liner from the same material in the shape of a brick 6 × 6 × 1 cm in size has been first prepared. This liner was sintered in the same way as the tablets on a nickel liner, heated beforehand in order to bring about the oxidation of the surface. All the samples were sintered in the oven on this liner. Ready ceramic samples were then ground on a buff wheel to the required thickness.

Samples sintered once im the above described manner will be further called samples *A*. Besides, samples sintered twice (*B*), three times (*C*), and four times (*D*) were prepared in the following manner. Samples *A* have been pulverized in a porcelain mortar and the powder thus obtained has been sifted through a sieve of 10000 eyes/cm^2. From this powder tablets were formed under the same pressure as before and resintered under the same conditions. In a similar way were prepared the samples *C* out of the *B* ones, and the samples *D* out of the tablets *C*, with the difference that the sintering of the latter took place in slightly changed conditions. Namely, samples *D* remained in the oven for 130 hours, while the period of heating up to the highest temperature (1340°C) amounted to 72 hours. The samples remained 8 hours at peak temperature and the cooling process lasted 50 hours. The sintering was performed in an electric furnace of fire clay in the Fireproof Material Factory in Skawina.

The samples *A* and *B* differed distinctly at first sight. Samples *A* were light and brittle and microscopic observation showed clearly their porous structure. The samples *B* having the same size were much heavier and after being ground had a smooth surface. They had also a greater hardness. The more times the samples were sintered the harder they were and the more compact structure they possessed. Ceramic samples are, however, always a more or less porous material. As far as its dielectric properties are concerned the porous material can be regarded as a system of small particles of the given material, immersed in a medium of a different dielectric constant — the air. The dielectric constant of such a system will depend on many factors, such as the dielectric constant of the components, the shape of the „pores" filled with air, and the ratio of the volume of the air contained in the pores to the volume of the whole sample. Only the last of these factors can be established by direct measurements. Its measure is the so called „absolute porosity" determined by means of the following formula (Polish Ceramic Norms, 1936)

$$P\% = \left(1 - \frac{d_v}{d}\right) 100$$

where $d_v = m/v$ is equal to the ratio of the mass of the dry sample (m) to the volume of the sample (v), determined by means of a hydrostatic balance after its previous saturation with water, and d is the density of the material out of which the sample was made, determined picnometrically after its pulverization.

Porosity measurements of the examined samples gave the following results:

Samples	*P*%
A	61
B	20
C	19
D	11,7

Method of measurements of the dielectric constant and of the dielectric losses

The measurement of capacity was made by means of a specially elaborated resonance method, which permitted to carry out the capacity measurements with a great accuracy even at high losses of the measured condensers, as well as to determine the dielectric losses.

A diagram of the equipment is shown in Fig. 1. The crystal oscillator I of frequency 5 MHz acts by induction on circuit II set up for resonance. The coupling bet-

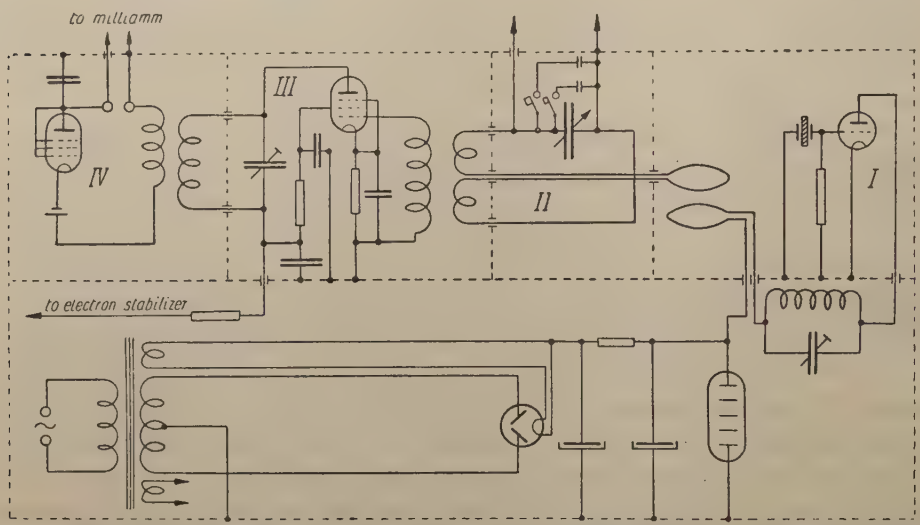

Fig. 1. Apparatus for measuring the dielectric constant. I — crystal oscillator, producing vibrations of frequency 5 MHz, II — resonance circuit, III — resonance amplifier, IV — rectifying circuit connected to the milliamperemeter

ween these circuits was extremely weak in order that the resonance curve be as little deformed as possible, and that the voltages in the resonance circuit be as low as possible. It was proved that at tuning the resonance circuit does not influence significantly the intensity of oscillations in the oscillator circuit. The coupling between the circuits was purely magnetic. All parts of the circuit which could have appreciable variable voltages have been taken away as far as possible and carefully screened. The voltage on the coatings of the variable condenser in the resonance circuit measured with the help of a valve voltmeter reached, at resonance, the value of 4,5 V, when there were no losses in the circuit.

As oscillations in the resonance circuit must have been very weak, a single lamp resonance amplifier (III) was used for determining the resonance. The resistance circuit acted purely by induction on the grid cathode circuit of the resonance amplifier, whereas the circuit which is in the anode circuit of the amplifier, tuned to the

generator frequency, acted purely by induction on the aperiodic circuit IV, which contained a rectifier lamp and a milliamperemeter. Individual circuits interacted on one another only by means of coupled coils. In order to avoid the action of individual circuits upon other circuits, the whole equipment has been mounted in an iron-plate box with double walls, divided also by means of iron- plate walls into separate chambers. The walls have been marked on Fig. 1 with a dash-line. Outside the box there was only a knob rotating the variable condenser in the resonance circuit, a milliamperemeter and the lamps. A disc with a scale has been placed on the axis of the variable condenser. Through a small window in the upper wall of the box the rotation angles could be read. A nonius placed close to the scale enabled the reading of the tenths parts of a scale division. Particular investigations showed that each of the circuits acted only on that circuit with which it was directly coupled.

The measurement consisted (1) in reading the two capacities of the variable condenser with disconnected test condenser, while the deflexions at both sides of the resonance point are equal, (2) the same readings after the test condenser has been switched in the circuit, while the deflexions of the amperemeter are the same as before. Subtracting from the sum of the two former figures the sum of the two latter, we obtain the double value of the condenser capacity in degrees of the scale of the variable condenser. The result obtained is independent of the conductivity and of the losses of the test condenser (Jeżewski 1927, 1933). The variable condenser possessed a capacity varying from the initial capacity C_0 to $C_0 + 100$ pF. As the capacity of the test condenser with $BaTiO_3$ samples exceeded, near the Curie point, the value of 100 pF, the scale of the variable condenser has been raised by connecting to it in parallel two constant condensers: 50 pF and 100 pF. Owing to these additional condensers it was possible to measure capacities up to 250 pF. The additional condensers were switched on in the circuit by means of pin-switches, excluding any capacity variations due to displacement of any parts with respect to one another.

When a condenser with losses has been switched on, the resonance curve was lowered. Losses were established by measuring the resistance connected in parallel to the variable condenser, which caused identical lowering of the maximum of the resonance curve. On account of the small sensitiveness of the resonance curve to resistances of about 1 megohm, this method, inaccurate at low losses, becomes more accurate at higher ones. In the case of resistances of, say, 1 megohm, the accuracy of measurements amounted to about 20%, at resistances of, say, 10 kΩ (which corresponds with the losses of the examined samples near the Curie point) it reached 1%.

As the absolute value of the dielectric constant had to be exactly measured, and not only its relative changes, a plate condenser with three electrodes with its outer coatings earthed has been used for the measurements. In such a condenser the inner coating is well screened by the outer ones, due to which the influence of the stray capacities in respect to the surrounding space is insignificant (Jellonek 1953). For calculating the capacity of the condenser filled with air, the following formula

has been employed (Kohlrausch, *Praktische Physik*),

$$C = \frac{r^2}{2a} + \frac{r}{\pi}\left[2\ln 2 + 2f\left(\frac{d}{4a}\right)\right],$$

where r is the radius of the circular inner coating, a — the thickness of the coatings, d — the thickness of the inner electrode (k). The capacity measurements could be carried out with an accuracy of 0,1 pF. Yet on account of the small accuracy in the calculation of the capacity of the condenser filled with air, which is dependent on the diameter of a very small inner coating as well as on the thickness of the tablets, one can hardly ascribe to the values of the dielectric constant a greater accuracy than 1%.

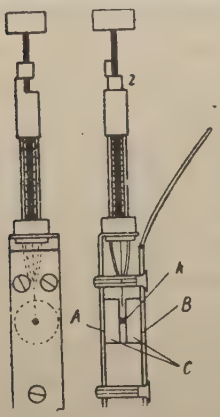

Fig. 2. Condenser for measuring the dielectric constant of the ceramic $BaTiO_3$. Plates A and B pressing the sample C, connected to the earthed coating of the variable condenser in the resonance circuit, k — inner electrode, z — stopper of the pin, switching on the test condenser in the circuit

The technical details of the condenser used, are shown in Fig. 2. Metal plates A and B pressed together two $BaTiO_3$ tablets (C), of equal size, silver-plated on their whole surfaces adjacent to the plates, while on their inner side there were silver electrodes having the shape of circles of about 0,6 mm in diameter. Between these electrodes there was a brass disc having the same diameter as the electrodes. Plates A and B were connected to the earthed coating of the variable condenser. The electrode k could be inserted in the circuit by means of a metal pin with a very thin edge. This rod could be raised and kept at constant distance from the inner coating by an adequate stopper (z). The tablets were silvered by means of firing samples covered with a silvering paste in suitable places.

Making tiny inner electrodes presented a particular difficulty. On account of the necessity of dealing with small capacities and simultaneously with regard to a very large value of the dielectric constant of the examined material, it was necessary to reduce the diameter of the inner coating below 1 mm. It was very difficult to silver such a small coating, which should have had exactly the shape of a regular circle. These technical difficulties have been surmounted in the following manner. By means of a cutter of a suitable diameter a cylindrical cavity about 0,2 mm deep was drilled in a prepared sample, the inside of the cavity was carefully silvered, fired in an oven and then the surface of the plate was slightly ground in order to remove the traces of silvering around the cavity. The coating was left a little sunk (0,1 mm), which enabled later on the central adjustment of the electrode k. The diameter of the electrodes was measured under the miscroscope by means of an eyepiece micrometer.

The test condenser was placed in an adequately built electric oven, whose temperature could be changed from room temperature up to temperatures above 200°C.

The temperature of the condenser was measured by means of a gradauted thermocouple, one junction of which touched the surface of the tablet. The second junction was held in ice. The temperature was measured with an accuracy up to 0,1°.

At such a high current frequency a marked influence of the inductance of the connecting wires upon the capacity measurements could be expected, the results of the measurements carried out by the resonance method were, therefore, compared with the results obtained by the accurate bridge method at a frequency of 4.5 kHz. The results of these measurements proved to be compatible. Thus it has been established that the influence of the inductance of the wires and condensers is smaller than the experimental errors. Evidently the inductances of the variable condenser in the resonance circuit together with the connecting wires, and the inductances of the test condenser compensated one another.

Results of the measurements

The results of the measurements of the dielectric constant as a function of the temperature were scheduled in Table I and in Fig. 3, and the results of the dielectric losses in Table II and in Fig. 4. As the differences in values of the losses for samples

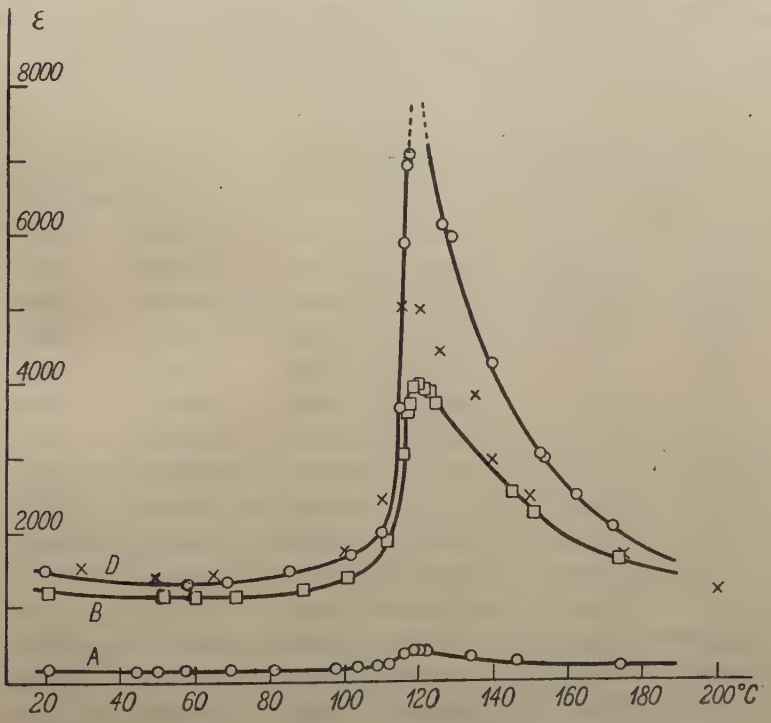

Fig. 3. Dieletric constants of samples *A*, *B*, and *D* of ceramic $BaTiO_3$ as functions of the temperature. Crosses indicate the values of the dielectric constant of the ceramic $BaTiO_3$ according to the measurements of Roberts

A, B and C lie within the limits of error, the values of the losses for samples B and C were not given here. Also for the sake of transparency of the drawing, the points representing the values of the dielectric constant of sample C, which do not differ considerably from the corresponding values for samples B, were not shown in Fig. 3.

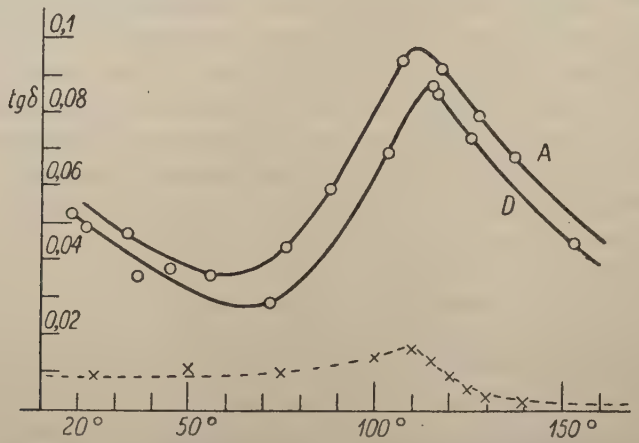

Fig. 4. tan δ for samples A and D of the ceramic $BaTiO_3$ as functions of the temperature. Crosses indicate the losses according to the measurements of Roberts

Table I

A t°C		B t°C		D t°C	
21,0	129	21,0	1190	20,0	1475
44,5	120	51,5	1104	58,0	1280
50,0	119	60,0	1108	68,7	1285
57,7	119	71,25	1124	85,0	1446
69,5	120	89,0	1184	101,5	1661
81,0	123	100,6	1353	110,0	1895
97,5	138	111,0	1850	115,0	3615
103,5	146	114,7	3014	116,0	5780
109,0	147	116,0	3643	117,0	6920
112,0	188	117,0	3686	117,5	7051
116,0	318	119,0	3923	126,0	6100
119,2	372	120,0	3918	128,7	5975
120,5	365	121,5	3860	139,7	4240
122,0	349	124,5	3725	152,5	3015
134,0	272	125,0	3680	154,0	2980
146,7	218	145,0	2502	162,2	2430
174,5	154	173,5	1612	172,2	2045

Table II.

A		*D*	
t°C	tan. δ	t°C	tan. δ
18,0	0,052	22,0	0,049
33,0	0,047	36,0	0,035
55,5	0,036	45,0	0,038
76,0	0,043	72,0	0,028
87,5	0,059	103,5	0,069
107,0	0,094	115,5	0,087
118,0	0,092	116,0	0,085
127,5	0,079	125,5	0,073
137,5	0,068	153,0	0,044

Conclusions

From the figures above, as well as from the Figs. 3 and 4 it is easy to prove that the way of preparing and the time of sintering the samples has, in general, no influence on the character of the dependence on temperature of the dielectric constant and the losses of the ceramic $BaTiO_3$. According to the results of investigations of the majority of authors, with increasing temperature, the dielectric constant, decreases at first from room temperature upwards, reaching a flat minimum at a temperature of about 60°C, then, from about 110°C it increases rapidly, reaching a maximum at the Curie point, which for all examined samples possesses the same value (within the limits of accuracy of measurements in the interval of 119,5°—120°C). The values of the dielectric constants of all samples decrease above the Curie point, but the slope of the curve is much smaller than below the Curie point. For comparison the results of the measurements of Roberts (1949) have been marked with crosses in Fig. 3, and it can be seen that they usually fall between the results for our samples *B* and *D*.

As can be seen from Fig. 4, the losses show a somewhat similar temperature dependence. Starting from room temperature, the losses decrease first with increasing temperature, reaching a minimum between 60° and 70°C, and later on they increase, reaching a maximum below the Curie point. For various samples this maximum lies at somewhat different temperatures. From Fig. 4 it can be seen, however, that this maximum comes nearer the Curie point for samples having a more compact structure (sample *D*). The influence of the way of preparing and the time of sintering the samples on the values of losses is rather small. Samples sintered many times do not show much smaller losses than samples sintered fewer times. On the same Fig. 4 the results of the measurements of Roberts (1947) made at a frequency of 1 MHz are indicated with crosses. The dependence on the temperature has the same character, but the numerical values are much smaller. Data of other authors lie nearer to ours. (Powles 1948, Siniakow 1951, Kazarnovskij 1951). In the case of dielectric

losses, there seems that, apart from the technique of preparing the samples, some impurities play here a decisive part, as well as the dependence on the current frequency and the test field strength. This problem will be the subject of further investigations.

Though the technique of the preparation of samples has a relatively small effect on the value of losses, yet it influences very obviously the values of the dielectric constant. This is illustrated in Table III, where the results of the measurements of the dielectric constant at 20°C ($\varepsilon_{20°}$) and at the Curie point (ε_c) for different samples are shown. For samples *D* only the order of magnitude has been given, for its value at the Curie point increased so remarkably, that the scale of the apparatus was insufficient to make a measurement possible. The values of the dielectric constant for samples *C* have been also included in the Table.

Table III

	$\varepsilon_{20°}$	ε_c	P%
A	129	380	61
B	1196	3940	20
C	1275	4685	19
D	1475	>7000	11,7

As may be seen from the Table above, the values of the dielectric constant for various samples differ very considerably, in spite of the fact that the material used for preparing the samples was identical. Also during the sintering process no impurities could enter the samples, because the latter, as was already mentioned, were sintered on a liner made of the same material. The dielectric constant increases with increasing number of sinterings and the time of their duration. At room temperature the dielectric constant of samples *B* is almost 10 times greater than that of samples *A* and the dielectric constant of samples *D* — about 25% greater than that of samples *B*. At the Curie point the dielectric constant of samples *B* surpasses more than ten times that of samples *A*, and the dielectric constant of samples *D* almost twice that of samples *B*. Undoubtedly this result is partly due to porosity. At the present moment it is, however, impossible to establish whether only porosity plays here a part, or there occur also some other changes of the macroscopic structure. Yet the results obtained by us explain in an easy manner the discrepancies between the values of the dielectric constants of the ceramic $BaTiO_3$ met in the works of different authors.

We wish to express here our thanks to all who enabled us to execute the above investigations, namety to Professor Trzebiatowski, Professor Roliński., and the Kasprzak Institute in Warsaw for providing the necessary materials, to Professor Konarzewski and the Fireproof Materials Factory in Skawina for granting us ovens for sintering, and to Professor Krupkowski for allowing us to carry out the pressing of samples in his Institute.

КРАТКОЕ СОДЕРЖАНИЕ

Ежевский и Пэх, ЗАВИСИМОСТЬ ДИЭЛЕКТРИЧЕСКИХ СВОЙСТВ КЕРАМИЧЕСКОГО $BaTiO_3$ ОТ ТЕХНОЛОГИИ ИЗГОТОВЛЕНИЯ ОБРАЗЦОВ ПРИ ТОКАХ ВЫСОКОЙ ЧАСТОТЫ.

Исследована зависимость постоянной диэлектрической и потерь керамического $BaTiO_3$ от способа изготовления образцов. Разработана методика измерения диэлектрический постоянный материал с очень большими диэлектрическим постоянными при помощи токов высокой частоты, и методика измерения потерь. Приготовлено четыре группы образцов $BaTiO_3$, назначенных *A*, *B*, *C*, *D*. Каждая следующая получена была из предыдущей посредством основателнього раздробления, сжатия под прессом и вторичной агломерации при температуре около 1350° С. Последняя группа *D* находилась в агломерационной печи особенно долго, ибо вместе с нагреванием и охлаждением около 130 часов. Установлено, что постоянная диэлектрическая каждой следующей группы образцов, во всех температурах, гораздо больше постоянной диэлектрической предыдущей группы. Потеры образцов в ряду *A*, *B*, *C*, *D*, постоянно, но не особенно значительно, уменьшаются.

REFERENCES

Graf, R. G., *Ceramic Age*, December 16, (1951).

von Hippel, A., *Rev. Mod. Phys.*, **22,** 221 (1950).

Jellonek, A., *Prace Państwowego Instytutu Technicznego* Nr 10, 9 (1953).

Jeżewski, M., *Z. Phys.* **43,** 442 (1927); *Phys. Z.*, **14,** 88 (1933).

Kazarnovskij, D. M., *Elektrichestvo*, **2,** 40 (1954).

Mason, W. P. and Matthias, B. T., *Phys. Rev.*, **74,** 1622 (1954).

Merz, W. J., *Phys. Rev.*, **75,** 687 (1949).

Pająk, Z., *Postępy Fizyki*, **5,** 212 (1954).

Piekara, A., *Postępy Fizyki*, **1,** 163 (1950).

Polskie Normy — metody badań materiałów ogniotrwałych PN/C-1601, December 1936.

Powles, J. G., *Nature*, **162,** 614 (1948).

Roberts, S., *Phys. Rev.*, **71,** 890 (1947); **75,** 989 (1949).

Rżhanov, A. B., *Uspiekhi Fizicheskich Nauk*, **38,** 461, (1949).

Siniakov, E. W., Stafijchuk, E. A., and Siniegubowa, L. S. *Zh. eksper. teor. Fiz.* **21,** 1396 (1951).

Trzebiatowski, W., Wojciechowska J., and Damm, J., *Roczniki Chemii*, **26,** 12 (1952).

ANGULAR DISTRIBUTION OF DEUTERONS FROM ^{9}Be (p, d) ^{8}Be. II.*

By J. Dąbrowski and J. Sawicki

Institute of Physics, Polish Academy of Science, Warsaw

(Received May 3, 1955)

The formula for the Born approximation cross-section for the ^{9}Be (p, d) ^{8}Be pickup reaction obtained with the help of the „^{8}Be + neutron" model of the ^{9}Be nucleus is compared with the experimental data for 6,5 and 22 MeV protons. The best agreement is obtained for the ^{8}Be — neutron square well radius $r_0 = 5 \cdot 10^{-13}$ cm. The angular distributions for larger angles lie under the experimental curves mostly due to the compound state formation. The absolute values of the cross section obtained by taking into account the Coulomb correction seem to be too great because of the neglect of the ^{8}Be — proton interaction. Comparison with the results of the Butler approximation determines the limits of validity of this approximation. The same model of the ^{9}Be nucleus is applied for the calculation of the Born cross section for the ^{9}Be (d, t) ^{8}Be reaction. The results are compared with experiment for 7,7 MeV deuterons. The "^{8}Be + neutron" model of the ^{9}Be nucleus is discussed.

Introduction

The expression for the differential cross section for the pickup reaction ^{9}Be (p, d)^{8}Be was obtained in I with the help of the Born approximation and by neglecting the ^{8}Be — proton interaction. The complete integrations in the Born approximation matrix element leading to the final formula (I, 11) were possible due to the assumption of the "^{8}Be + neutron" model of the ^{9}Be nucleus in $P_{3/2}$ state with the square well ^{8}Be — neutron potential.

The aim of the present paper is to compare the results of our calculations with the experimental results of Cohen et al. (1953) and Harvey (1951). Thus it is the proof of the "^{8}Be + neutron" model from the point of view of the pickup (p, d) reaction. This model, it is well known, satisfactorily explained the electrodisintegration (Mamasachlisov 1943, Guth and Mullin 1949) and photodisintegration at low gamma quanta energy (Guth and Mullin 1949).

---

* This is the second part of the paper by Dąbrowski and Sawicki (1955a), which will be further referred to as I.

It is well known (Gerjuoy 1953) that the main feature of the Butler (1951) approximation is to cut off of a sphere of radius r_0 from the $\vec{r}_n$ integration domain in the Born formula[1]. In order to obtain the Butler expression for the differential cross section the first term in eq. (I, 9b) must be omitted the second (multiplied by N_a) being retained. This method of passing to the Butler expression was more convenient then that indicated by Daitch and French (1952, eq. (8)) being also simple in the case of the assumed square well ^{8}Be-neutron interaction. In the present paper the comparison with the results of the Born and Butler theory will be given. For the comparatively great proton energy $E_p = 22$ MeV used in experiments by Cohen et al. (1953) it is interesting because for the correspondingly large values of the momenta the domain $r_n < r_0$ becomes important.

The "^{8}Be + neutron" model of the ^{9}Be nucleus is also aplied to the ^{9}Be (d, t) ^{8}Be reaction using of the Born approximation. The results obtained are compared with the experimental results of Holt and Marsham (1953) and the theoretical curves of Newns (1952).

For both reactions the Coulomb correction is taken into account in the calculation of the absolute values of the cross section.

Numerical Results. Coulomb Corrections

The ^{9}Be square well potential was assumed to have the radius $r_0 = 5 \cdot 10^{-13}$ cm (the respective depth being $V_0 = 12{,}09$ MeV). This value is found most satisfactory in the theory of electrodisintegration and photodisintegration (Mamasachlisow 1943, Guth and Mullin 1949). Besides the values $r_0 = 3 \cdot 10^{-13}$ cm ($V_0 = 28{,}92$ MeV, and $r_0 = 7 \cdot 10^{-13}$ cm ($V_0 = 7{,}28$ MeV) are discussed. For the deuteron potential parameters we take the values $V_0 = 21$ MeV, $a = 2{,}82 \cdot 10^{-13}$ cm.

In order to compare our results with experiment we obtain the differential cross section in the laboratory frame $d\sigma_L/d\Omega_L$ with the help of the known formula (see e.g. Schiff 1949):

$$\frac{d\sigma_L}{d\Omega_L} = \frac{[1 + \bar{\gamma}^2 + 2\bar{\gamma}\cos\Theta_s]^{3/2}}{1 + \bar{\gamma}\cos\Theta_s} \frac{d\sigma_s}{d\Omega_s}, \tag{1}$$

where

$$\gamma = \frac{v_s}{v_d} = \frac{2}{9}\frac{k_p}{k_d}. \tag{1a}$$

v_s is the center of mass velocity and v_d is the velocity of the deuteron in the c. m. system. The scattering angle Θ_L in the laboratory frame is connected with the c. m. system scattering angle Θ_S by

$$\operatorname{tg}\Theta_L = \frac{\sin\Theta_s}{\gamma + \cos\Theta_s}. \tag{1b}$$

[1] The same symbols will be used as in I.

In Fig. 1 the angular distribution of deuterons from the ^{9}Be (p, d) ^{8}Be reaction calculated from (I, 11) for $r_0 = 5 \cdot 10^{-13}$ cm is compared with the experimental results of Cohen et al. (1953) and Harvey (1951).

In Fig. 2 the comparison of our angular distributions for $r_0 = 3, 5, 7 \cdot 10^{-13}$ cm with the data of Cohen et al. (1953) is given. In Fig. 2 the Butler theory angular distributions are also given for the same values of r_0.

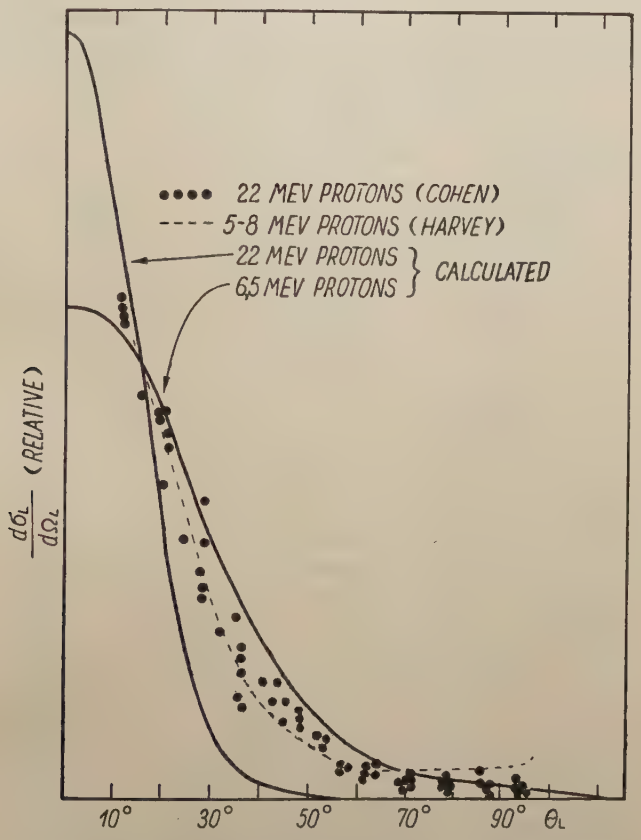

Fig. 1. Angular distribution of deuterons from the ^{9}Be (p, d) ^{8}Be (ground state) reaction. The experimental points are taken from Cohen et al. (1953)

In Fig. 3 analogous curves are compared to the experimental data of Harvey (1951).

The eq. (I, 11) makes it possible to calculate the absolute values of the cross section. However it is known, that the Coulomb effect lowers these values very definitely (Yoccoz 1954, Sawicki 1955). The most important role is played here by the normalization factor of the Coulomb wave functions. The Coulomb effect on the angular distribution is merely to give some flattening of the curves. In the present paper we shall confine ourselves to the estimate of the Coulomb effect on the absolute values of the cross section. In eq. (I, 11) the plane waves $e^{i\vec{k}_p\vec{r}_p}$, $e^{-i\vec{k}_d\vec{r}_d}$ were used to represent the

incident proton and the scattered deuteron. On taking into account the Coulomb effect the plane waves should be replaced by the respective Coulomb functions (see e. g. Schiff 1949). The main influence of the Coulomb effect on the absolute values of the cross section comes from the factor

$$F = \left(\frac{2\pi n_p}{e^{2\pi n_p} - 1}\right)\left(\frac{2\pi n_d}{e^{2\pi n_d} - 1}\right) \tag{2}$$

equal to the product of the ratios of the squares of the Coulomb functions and the respective plane waves (at the zero values of the arguments). In eq. (2) $n_p = 4e^2 M_p^* / \hbar^2 k_p$

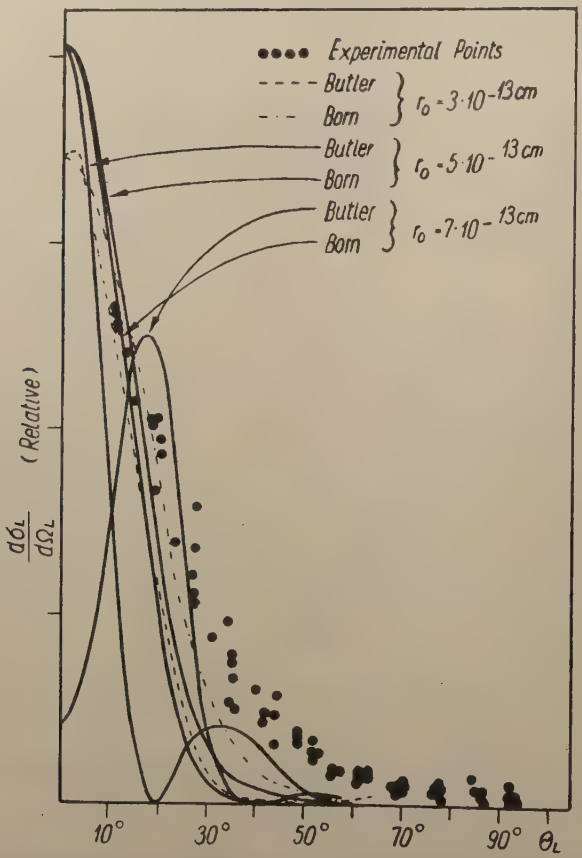

Fig. 2. Angular distribution of deuterons from the ^{9}Be (p, d) ^{8}Be (ground state) reaction for 22 MeV protons. The experimental points are taken from Cohen et al. (1953)

$n_d = 4e^2 M_d^* / \hbar^2 k_d$. Thus the Coulomb effect will be taken into account by multiplying the absolute values of the cross section calculated from (I, 11) by the Coulomb correction factor F. The respective values of this factor are:

$$F = \begin{cases} 0{,}132 \text{ for } E_p = 6{,}5 \text{ MeV}, \\ 0{,}344 \text{ for } E_p = 22 \text{ MeV}. \end{cases} \tag{3}$$

In Table I the absolute values of the differential cross section for $\Theta_L = 0$ are given with F being taken into account.

Discussion of the Results

From Fig. 1 it is seen that the angular distributions for $r_0 = 5 \cdot 10^{-13}$ cm are similar to the experimental ones. This comparison is not quite complete because of the lack of experimental data for small scattering angles. However for proton energy $E_p = 22$ MeV the theoretical curve falls off too rapidly with increasing scattering

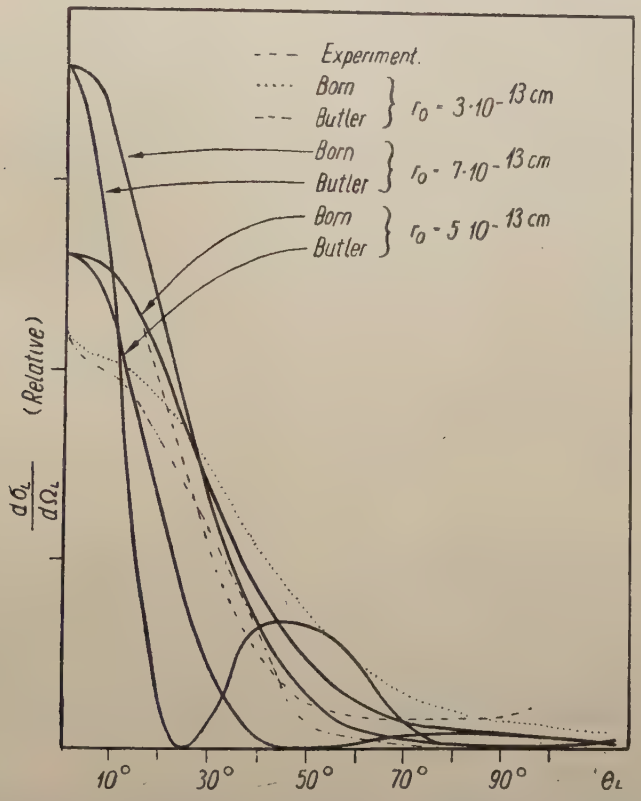

Fig. 3. Angular distribution of deuterons from the ^{9}Be(p, d)^{8}Be (ground state) reaction for 6,5 MeV. protons. The results of Harvey's experiments for $E_p = 5, 6, 7, 8$ MeV (mean value 6,5 MeV) are taken from Cohen et al. (1953).

angles. It is the common feature of stripping reactions probably resulting from the continuous background given by the compound state mechanism.

From Fig. 2 it is seen that an increase in r_0 to the value $7 \cdot 10^{-13}$ cm gives for $E_p = 22$ MeV much too steep a Born approximation angular distribution, and the value $r_0 = 3 \cdot 10^{-13}$ cm gives a somewhat better agreement with the experimental angular distribution.

On the other hand from Fig. 3 we see, that for $E_p = 6{,}5$ MeV the value $r_0 = 3 \cdot 10^{-13}$ cm gives too flat a Born angular distribution. Conversely the value $r_0 = 7 \cdot 10^{-13}$ cm yields an agreement similar to that for $r_0 = 5 \cdot 10^{-13}$ cm (however for large scattering angles the curve $r_0 = 7 \cdot 10^{-13}$ cm falls still faster than does that for $r_0 = 5 \cdot 10^{-13}$ cm).

Some flattening of the angular distributions would be obtained by taking into account the Coulomb effect (Yoccoz 1954, Sawicki 1955). On the other hand, however, the taking into account of the nuclear interaction ^{8}Be — proton gives some inverse effect (Horowitz and Messiah 1953).

The conclusion is that the value $r_0 = 5 \cdot 10^{-13}$ cm gives comparatively the best agreement of the theoretical and experimental angular distributions. Thus the simple "^{8}Be + neutron" model of the ^{9}Be nucleus proposed by Mamasachlisow (1943) and then used by Guth and Mullin (1949) receives new confirmation. Apparently the Born approximation of the pickup reaction is crude and thus the importance of this confirmation is limited. It would be very interesting to compare our calculations with further experimental data announced by Reynolds and Standing (1954).

Let us come now to the comparison of the results of the Born and Butler theories. From Fig. 2 it is seen that the Butler theory curves for $E_p = 22$ MeV are in disagreement with the experimental data. This disagreement is the greater the larger is r_0. The fact that the Butler theory is not suitable for the pickup reaction at high energies was mentioned by Selove (1955)[2], who explains this fact too. Namely the Butler approximation relies upon the modification of the integral

$$\int d\vec{r}_n \, e^{-i\vec{k}\vec{r}_u} R(r_n) \Phi_{m_i} \tag{4}$$

by the removal of the integration domain $r_n < r_0$. We see, that for $E_p = 22$ MeV k takes on values from $0{,}415 \cdot 10^{13}\text{cm}^{-1}$ for $\vartheta_s = 0$ and for $\vartheta_s = 60°$ $k = 1{,}09 \cdot 10^{13}\text{cm}^{-1}$ corresponding to the wavelengths $2\pi/k = 15{,}1 \cdot 10^{-13}$ cm and $5{,}6 \cdot 10^{-13}$ cm respectively. The wavelengths are of the order of r_0 and thus the contribution from $r_n < r_0$ has significant influence on the value of the Fourier transform (4). Thus the removal of this domain from (4) gives results disagreeing with experimet. For $E_p = 6.5$ MeV the wavelenghts mentioned are equal $24{,}4 \cdot 10^{-13}$ cm for $\Theta_s = 0$ and $10{,}2 \cdot 10^{-13}$ cm for $\Theta_s = 60°$. Here these wave lengths are greater than r_0 yet not enough, especially for $r_0 = 7 \cdot 10^{-13}$ cm, to justify the removal of the domain $r_n < r_0$ from integral (4). In Fig. 3 it is seen that for $E_p = 6{,}5$ MeV and $r_0 = 7 \cdot 10^{-13}$ cm the Butler theory curve is in disagreement with the experimental curve. For smaller r_0 the Butler curves become more like the Born curves, but have zeros of angular distribution which do not exist in the experimental data (compare Daitch and French 1952).

Thus the Butler approximation should be treated as a way of avoiding diffuculties resulting from lack of knowledge of the nuclear wave functions in the interior of the

[2] The authors are much indebted to Dr W. Selove for letting them see his results prior to publication.

nucleus in the general case. This way is justified only if the internal domain has little importance for the values of the Born integrals. It is then not applicable to higher energies, for which on the other hand the application of the Born approximation is the more justified.

This fact, visible in the results of our calculations (Fig. 2, Fig. 3), shows the failure of the suggestion of Cohen et al. (1953) to compare the experimental data with the

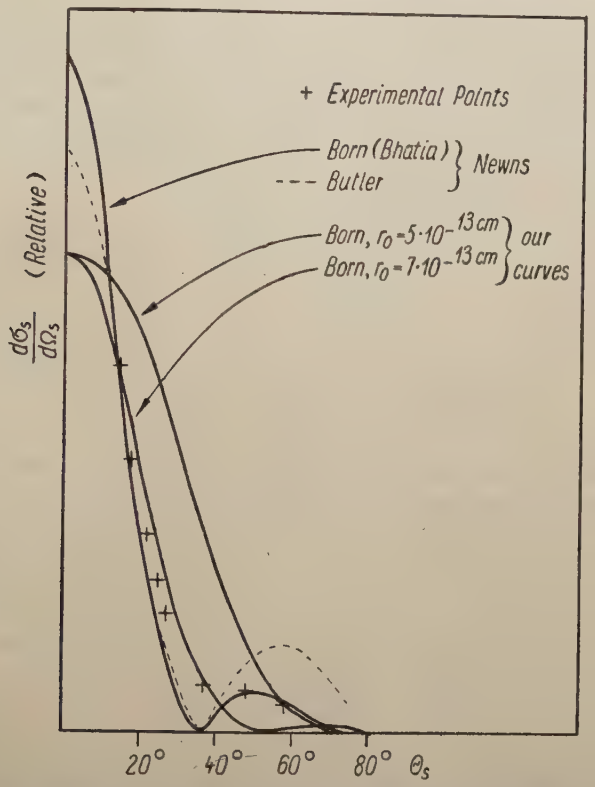

Fig. 4. Angular distribution of tritons from the ^{9}Be(d, t)^{8}Be (ground state) reaction for 7,7 MeV deuterons. The experimental points of Holt and Marsham and the Butler and Bhatia curves are taken from Newns (1952)

Butler theory. The result given by the Born approximation is the explanation of the general resemblance of the angular distributions for $E_p = 6{,}5$ MeV and for $E_p = 22$ MeV. This result was hard to explain by the Butler theory.

As concerns the absolute values of the cross sections there is a lack of experimental data. One can only guess from the mention by Harvey (1951), that the value of the cross section for $E_p = 5 - 8$ MeV is 0,024 barn/steradian for $\Theta_L = 20°$. The corresponding theoretical value for $r_0 = 5 \cdot 10^{-13}$ cm is 0,26 barn/steradian i.e. about 11 times too great. However it is known from the paper by Horowitz and Messiah (1953), that the application of the nuclear ^{8}Be — proton interaction would lower the absolute value

of the cross section. In the cases investigated Horowitz and Messiah found a decrease by a factor 2 — 6. It is thus hoped that in our case the application of the interaction mentioned may lead to agreement between theory and experiment. It is worth while to notice, that apparently the Butler formulas give smaller absolute values. These values are not discussed here because of the disagreement of the Butler angular distribution with experiment[3].

Table I. Absolute values of $(d\sigma_L/d\Omega_L)\,\Theta_L = 0$ in barn/steradian for the ^{9}Be (p, d) ^{8}Be (ground state) reaction. The Coulomb correction is taken into account. Asterisks denote cases in which the angular distribution is in distinct disagreement with experiment

r_0 in 10^{-13}cm	$E = 6{,}5$ MeV		$E = 22$ MeV	
3	0,291	0,213	0,512	0,288
5	0,347	0,134	0,491	0,058*
7	0,420	0,054*	0,412	0,005*
	Born	Butler	Born	Butler

The ^{9}Be (d, t) ^{8}Be Reaction

This reaction was investigated by Newns (1952) with the help of the Butler theory and the Born theory with the approximation of Bhatia et al. (1952). Now we investigate this reaction with the help of the exact Born approximation with the application of the "^{8}Be + neutron" model of the ^{9}Be nucleus.

On neglecting the ^{8}Be — deuteron interaction and the Coulomb effect we obtain for the differential cross section in the c. m. system the final result:

$$\frac{d\sigma_s}{d\Omega_s} = \frac{M_t^* M_d'^*}{(2\pi\hbar^2)^2}\frac{k_t}{k_d}\pi I_q^2 I_p^2, \tag{5}$$

where $M_t^* = (24/11)M$, $M_d'^* = (18/11)M$ are the respective triton and deuteron reduced masses, k_t and k_d are the respective momenta,

$$I_q = \sqrt{\frac{\pi}{2}}\, V_0 \int_0^{r_0} dr_n\, r_n^2 R(r_n)\, I_{3/2}(qr_n)/\sqrt{qr_n}, \tag{6}$$

where $q = (8/9)\,\vec{k}_d - \vec{k}_t$ and

$$I_p = \int d\vec{u}\, d\vec{s}\, e^{-i\vec{p}\,\vec{s}}\, \chi_t(u, s)\, \psi\left(\frac{2}{\sqrt{3}}\, u\right), \tag{7}$$

[3] It is seen from Table I, that the absolute values of the cross section are comparatively little sensitive to the values of r_0, contrary to the suggestion of our preliminary note (Dąbrowski and Sawicki 1954).

where $\vec{p} = \vec{k}_d - (2/3)\vec{k}_t$; $\vec{s} = \vec{r}_d - \vec{r}_n$, $\vec{u} = (\sqrt{3}/2)\,\vec{\varrho}$ are internal coordinates of the triton; $\chi_t(u, s) = N_t e^{-2\gamma^2(u^2+s^2)}$ is the internal wave function of the triton used by Newns (1952) and $\psi(\varrho) = N_H(e^{-\beta\varrho} - e^{-\Gamma\varrho})/\varrho$ is the internal Hulthen wave function of the deuteron with the parameter values used e. g. by Malenka et al. (1953).

The numerical computations were performed for $r_0 = 5 \cdot 10^{-13}$ cm and $7 \cdot 10^{-13}$ cm for the incident deuteron energy $E_d = 7{,}7$ MeV. Unfortunately unlike the (p, d) reaction the angular distribution was obtained for $r_0 = 5 \cdot 10^{-13}$ cm much too flat; for $r_0 = 7 \cdot 10^{-13}$ cm the agreement with the experimental data of Holt and Marsham (1953) is better (see Fig. 4).

To estimate the absolute values of the cross section similarly as for the (p, d) reaction the Coulomb factor

$$F = \left(\frac{2\pi\, n'_d}{e^{2\pi n'_d} - 1}\right)\left(\frac{2\pi\, n_t}{e^{2\pi n_t} - 1}\right), \tag{8}$$

where $n'_d = 4e^2\, M^*_d/\hbar^2 k_d$, $n_t = 4e^2\, M^*_t/\hbar^2 k_t$ was applied.

For $E_d = 7{,}7$ MeV $F = 0{,}11$ and the respective values of $\left(\frac{d\sigma_s}{d\Omega_s}\right)_{\Theta_s=0}$ are 87,12 mb/ster and 72,30 mb/ster respectively for $r_0 = 5 \cdot 10^{-13}$ cm and $r_0 = 7 \cdot 10^{-13}$ cm. The respective total cross sections σ_t are 110,9 mb and 50,6 mb as compared with the experimental value given by Wolfgang and Libby(1952) $\sigma^t = 230$ mb. Unlike the ^{9}Be (p, d) ^{8}Be reaction, the absolute values of the cross section obtained are smaller than the respective experimental value. In the similar case of the ^{6}Li (n, t)^4 He reaction the absolute values of the theoretical cross section were also small as compared to the common feature of the absolute values of the cross section in stripping (Dąbrowski, Sawicki 1955).

Remarks Concerning the Model of the ^{9}Be Nucleus

It is well known that in general the shell (two body) model of the ^{9}Be nucleus is very crude and does not explain many processes and properties of this nucleus (e. g. its magnetic moment). For a description of them a more accurate model "$2\alpha + n$" ought to be used.

However the mechanism of the ^{9}Be (p, d) ^{8}Be and ^{9}Be (d, t) ^{8}Be reactions like the mechanism of the ^{9}Be (γ, n) ^{8}Be reaction pretty well distinguishes the external neutron and indicates the use of the shell model. The fact that the external neutron in the ^{9}Be nucleus is loosely bound with the energy 1,63 MeV compared with 8 — 10 MeV average binding energy per particle, is visualised in the large values of the cross sections for the (p, d) and (d, t) reactions.

However it is necessary to mention, that recently the "^{8}Be+neutron" model was questioned in the case of photodisintegration even for γ — quanta energy 6 MeV by Carver et al. (1954). Their experiments suggest, that only 20% of the ^{8}Be nuclei from the ^{9}Be (γ, n) ^{8}Be reaction are produced in the ground state. In the remaining cases appear ^{8}Be (in an excited state) and ^{5}He in the ratio 1,2:1. Apparently in both the

(p, d) and (d, t) reactions the competing mechanism does not interfere with the production of ^{5}He. Similarly the reaction leading to ^{8}Be* is eliminated by the proper selection of scattered particle energy (e. g. Cohen 1953, Holt and Marsham 1953).

Further the theory of the (γ, n) reaction with the use of the "^{8}Be + neutron" model given by Überall (1953) for large γ — quanta energy 20 MeV $< E_\gamma <$ 200 MeV was found to be in complete disagreement with experiment (Jones and Terwilliger 1953). Similarly the "^{8}Be + neutron" model may be less important for large energies E_p and E_d. However for the energies $E_p = 6{,}5$; 22 MeV and $E_d = 7{,}7$ MeV the agreement with experiment was found satisfactory for $r_0 = 5 - 7 \cdot 10^{-13}$ cm. The best value seems to be $r_0 = 5 \cdot 10^{-13}$ cm.[4].

We are much indebted to Prof. L. Infeld and Prof. W. Rubinowicz for a helpful discussion and their kind interest in this work, and to Mr. W. Czyż for interesting discussions.

APPENDIX

On the Born Formula for the Cross Section

We shall give an outline of the deduction of the Born cross section in the c. m. system for the ^{9}Be (p, d) ^{8}Be reaction in order to explain the simplifying assumptions used in this deduction.

The hamiltonian of the system H may be written down in two forms

$$H = H_9(\xi \vec{r}_n \sigma_n) + V_d + T_{\vec{r}_p} = H_8(\xi) + H_d(\vec{\varrho}\, \sigma_n \sigma_p) + V_0 + T_{\vec{r}_d}. \quad (1A)$$

H_9, H_8, H_d are respectively the internal Hamiltonians of the ^{9}Be, ^{8}Be nucleus and the deuteron. $T_{\vec{r}_p}$, $T_{\vec{r}_d}$ are respectively the kinetic energy operators of the systems: proton — ^{9}Be nucleus and deuteron — ^{8}Be nucleus. V_d, V_0 are the proton — neutron and ^{8}Be — neutron interaction potentials. In (1A) the ^{8}Be — interaction potential is neglected.

We try to solve the Schrödinger equation of the problem

$$H\psi = E\psi \quad (2A)$$

in the form

$$\psi = \psi_0 + \psi_1, \quad (3A)$$

where ψ_0 is the plane wave of the proton incident on ^{9}Be and ψ_1 represents the deuteron departing from the ^{8}Be nucleus.

On substituting (3A) in (2A) we find with respect to (1A):

$$(H_8 + H_d + T_{\vec{r}_d} + V_0 - E)\,\psi_1 = -V_d\,\psi_0. \quad (4A)$$

[4] Although the value $r_0 = 7 \cdot 10^{-13}$ cm gives a better agreement with experiment than the value $r_0 = 5 \cdot 10^{-13}$ cm for the angular distribution for the (d, t) reaction, the value gives a better value for the total cross section for the same reaction.

The potential V_d is contained in H_d and thus on the left hand side of (4A) we have $(V_d + V_0)\,\psi_1$. The first Born approximation rejects, the term[5] $V_0\psi_1$. Thus we neglect the term $V_0\psi_1$ as compared to $V_d\,\psi_1$. This corresponds to the mechanism of the (p, d) reaction, in which the neutron is picked up from the ^{9}Be nucleus due to the V_d potential and in spite of the V_0 potential. Besides the $n - p$ interaction is stronger than the n — ^{8}Be (greater binding energy). It seems that taking the term $V_0\,\psi_1$ into account would lower the cross section[6]. It is however beyond the first Born approximation.

On neglecting V_0 in (4A) we can calculate ψ_1 in the usual way and then the cross section.

It is interesting, that in the calculation of the cross section for the inverse ^{8}Be (d, p) ^{9}Be reaction V_d is neglected as compared with V_0 in the equation analogous to (4A). Notwithstanding this both the cross sections are connected with the "reciprocity theorem for nuclear reactions". The validity of this theorem for the Born approximation can easily be proved explicitly (Bransden 1954).

КРАТКОЕ СОДЕРЖАНИЕ

Домбровский и Савицкий. УГЛОВОЕ РАСПРЕДЕЛЕНИЕ ДЕЙТРОНОВ С РЕАКЦИИ ^{9}Be(p,d)^{8}Be II.

Полученный при помощи модели „^{8}Be+нейтрон" формулы эффективного сечения в приближении Борна для реакции „pickup" ^{9}Be(p,d)^{8}Be сравнено с опытными данными для протонов с энергией 6,5 и 22 MeV. Самую лучшую согласованность получено для прямоугольной ямы потенциала „^{8}Be+нейтрон" с радиусом $r_0 = 5.10^{-13}$ см. Угловое распределение для больших углов лежит под экспериментальными кривыми главным образом благодаря образованию сложеных состояний. Абсолютные значения эффективного сечения, полученные учитывая куломбовскую коррекцию, кажутся чересчур большими по причине упущения из виду взаимодействия ^{8}Be и протона. Сравнение с результатами, полученными на основании приближения Батлера, определяет предел применимости этого приближения.

Эту же самую модель ядра ^{9}Be применено при вычислении борновского эффективного сечения реакции ^{9}Be(d,t)^{8}Be. Результаты сравнено с опытом для дейтронов с энергией 7,7 MeV. Придискутирована модель ядра ^{9}Be „^{8}Be+нейтрон".

REFERENCES

Bhatia, A. B., Huang, K., Huby, R. and Newns, H. C., *Phil. Mag.*, **43**, 485 (1952).
Bransden, B. H., *Phys. Rev.*, **94**, 726 (1954).
Butler, S. T., *Proc. Roy. Soc.*, **208**, 559 (1951).
Carver, J. H., Kondaiah, E. and Mc Daniel, B. D., *Phil. Mag.*, **45**, 948 (1954).

[5] It is equivalent to the substitution in the integral equation for ψ of a plane wave in place of ψ.

[6] In our preliminary note (Dąbrowski, Sawicki 1954) in the discussion of this question the known fact was not mentioned, that the interaction p — ^{8}Be gives a considerable reduction in the values of the cross section (Horowitz and Messiah 1953). Moreover it was not mentioned that the „neglect" of V_0 as compared with V_d is equivalent to the Born approximation.

Cohen, B. M., Newman, E., Handley, T. H. and Timnic, A., *Phys. Rev.*, **90,** 323 (1953).
Daitch, P. B. and French, J. B., *Phys. Rev.*, **87,** 900 (1952).
Dabrowski, J. and Sawicki, J., *Nuovo Cimento*, **12,** 293 (1954); *Acta phys. Polon.*, (1955a) in print; *Phys. Rev.*, **96,** 1002 (1955b).
Gerjuoy, E., *Phys. Rev.*, **91,** 645 (1953).
Guth, E. and Mullin, C. J., *Phys. Rev.*, **76,** 234 (1949).
Harvey, J. A., *Phys. Rev.*, **82,** 298 (1951).
Holt, J. R. and Marsham, T. N., *Proc. Phys. Soc.* [London], **66,** 1032 (1953).
Horowitz, J. and Messiah, A. M. L., *J. Phys. Radium*, **14,** 695 (1953)
Jones, L. W. and Terwilliger, K. M., *Phys. Rev.*, **91,** 699 (1953).
Malenka, B. I., Kruse, U. E. and Ramsey, N. F., *Phys. Rev.*, **91,** 1162 (1953).
Mamasachlisov, V. I., *J. Phys. U. S. S. R.*, **7,** 239 (1943).
Newns, H. C., *Proc. Phys. Soc.* [London], **65,** 916 (1952).
Reynolds, J. B. and Standing, K. G., *Phys. Rev.*, **95,** 639 (1954).
Sawicki, J., *Bull. Acad. Polon. Sci., Cl.* III, (1955), in print.
Schiff, L. I., *Quantum Mechanics*, N. York, 1949.
Selove, W., (1955), in print.
Überall, H., *Z. Naturforsch.*, **8a,** 142 (1953).
Wolfgang, R. L. and Libby, W. F., *Phys. Rev.*, **85,** 437 (1952).
Yoccoz, J., *Proc. Phys. Soc.* [London], **67,** 813 (1954).

ELECTRONIC INTERACTION IN THE FREE-ELECTRON MODEL FOR NON-BRANCHED CONJUGATED SYSTEMS

By S. Olszewski

Institute of Physics, Polish Academy of Sciences, Warsaw

(Received May 30, 1955)

The ASMO CI method for molecular orbitals of a free-electron for non-branched bond systems of conjugated molecules is presented here in close analogy to the ASMO CI theory as developed by Goeppert-Mayer and Sklar and Craig for molecular orbitals in the form of the linear combination of atomic 2p orbitals. This scheme was used to calculate the energy levels in two cases: ethylene and butadiene. The results are in a better agreement with experimental data than those which can be obtained by analogical computations with LCAO MO method. This is the case especially in the singlet-triplet separation for the first excited states. In addition a significant decrease in the configurational interaction effect compared with the LCAO MO method was obtained.

1. The Theory

The theory of electronic spectra of unsaturated hydrocarbons in molecular orbitals (MO) formulation is generally used in two ways: the first is the linear combination of atomic orbitals (LCAO), (see e.g. Pullman and Pullman 1952), where the molecular orbitals are built from the atomic 2p orbitals of individual atoms. In the second one, a free electron (FE) model, we have the quantization problem of free electronic motion in a long thin tube extended along the molecular free-bond path. In these two methods the π-electrons are treated independently from the rest of the molecule which manifests itself only as an effective "core". It is in the field of this core that the π-electrons move. (Ruedenberg and Scherr 1953).

In the LCAO MO method in its simplest form the presence of the core is taken into account in the Coulomb and resonance integrals usually extrapolated from the experimental data. The FEMO method in the form as it is at present developed assumes the interaction potential of the core with π-electrons as constant. This potential may be taken as equal to zero. The only quantity taken from experiment in the latter method (and in the exact LCAO MO method as well) is the mean length of the bond between the carbon atoms in the conjugated systems of double bond.[1]

[1] Recently there appeared some papers which confirm a close correspondence between both FE and LCAO treatments (see e. g. Ruedenberg 1954). These results may be considered as a great support for our theory.

The next step in the LCAO MO method is to build the wave functions corresponding to the particular electronic configurations of a molecule. These wave-functions take the form of antysymmetrized products of molecular spin-orbitals (ASMO). At the same time in the Hamiltonian operator mutual electronic interaction terms are included. (Goeppert Mayer and Sklar 1938).

In order to determine the energy of the stationary states of the molecule as precisely as possible the configurational interaction (CI) is taken into account. The full π-electronic wave function of a molecule is built for a given state in the form of a linear combination of the eigenfunctions of the configurations, (Craig 1950).

In the calcultations all integrals may be computed by assuming only the $C - C$ distance as known. Thus a purely theoretical scheme of a consistent theory of electronic spectra for the molecules investigated is obtained. We shall call it further on the "exact LCAO MO method".

The aim of this work is to develop the theory of electronic spectra of unsaturated hydrocarbons by means of a free-electron model in a similar way to that of the conventional LCAO MO method. We shall carry it out first for a non-branched model. The generalization of the theory for a model describing branched bond path systems is in preparation.

The purpose of the free-electron theory is to solve the eigenproblem in the following form

$$H\varphi = E\varphi \tag{1}$$

$$\text{where} \quad H = -\frac{\hbar^2}{2m}\nabla^2 + V$$

which corresponds to the electronic motion in a box extended along the molecular core in rectangular coordinates.

We assume, as usual, that the potential is only dependent on the x bond path coordinate corresponding to the core, i.e.

$$V = V(x)$$

We assume further the size of the cross-section of the box to be small in comparison with its length. This means that the excitations energies in the y and z directions are much higher than in the x direction. Thus the movements in y and z remain in the ground state while that in x direction becomes excited. (Ruedenberg and Scherr 1953).

By this assumptions our problem has the three-dimensional solution: (Ruedenberg and Scherr 1953).

$$\varphi(x, y, z) = \psi(x)\,(^2/\varepsilon)\sin(\pi y/\varepsilon)\sin(^2\pi z/\varepsilon), \tag{2}$$

where ε is the size of the square cross-section of the box, and the following relations are fulfilled

$$0 \leqslant y \leqslant \varepsilon, \qquad -{}^1/_2\varepsilon \leqslant z \leqslant {}^1/_2\varepsilon, \qquad \varepsilon \ll l$$

x as before being the coordinate tangent to the path bond, y being normal to x in the

plane of the molecule, and z being normal to the plane of the molecule, which we take as $z = 0$. ψ represents the one-dimensional molecular orbital depending on x.

For a molecule containing s π-electrons moving along the core, the Hamilton operator takes the form

$$\mathcal{H} = \sum_{\mu} H^{\mu} + \frac{1}{2} \sum_{\mu \neq \nu} e^2 / r_{\mu\nu}, \tag{3}$$

where H^{μ} is the Hamiltonian (1) for the μ-th electron moving in the field of the core itself.

For the non-branched molecular model the π-electron motion along the broken line of the core (e.g. in polyens) can be approximated by the motion in a straight-linear box with a length equal to the free bond path length (see Ruedenberg and Scherr 1953, Fig. 2). Then we have

$$r_{\mu\nu} = \sqrt{(x_{\mu} - x_{\nu})^2 + (y_{\mu} - y_{\nu})^2 + (z_{\mu} - z_{\nu})^2} \tag{4}$$

The perturbations introduced by this assumption may be taken as insignificant and may be neglected (particularly for the all-trans case).

The wave functions of the s electron system are built from normalized antisymmetrized product functions of the type (Mulliken 1949)

$$\Phi_{\Lambda} = (s!)^{-1/2} \begin{vmatrix} (\varphi_1 \alpha)^1 (\varphi_1 \beta)^1 (\varphi_2 \alpha)^1 .. \\ (\varphi_1 \alpha)^2 (\varphi_1 \beta)^2 (\varphi_2 \alpha)^2 .. \\ \ldots\ldots\ldots\ldots\ldots\ldots \end{vmatrix}, \tag{5}$$

where Λ is the running index by which the correspondence of the electrons to the particular molecular orbital φ_n together with the spin function α or β is characterized. In other words, Λ denotes the spin-orbital configuration.

The energy of the electronic state corresponding to the wave function Φ_{Λ} takes the form (Mulliken 1949)

$$E_{\Lambda} = \sum_{n} I_n + \frac{1}{2} \sum_{nm} (J_{nm} - K'_{nm}) \tag{6}$$

(the summations runs over all occupied spin-orbitals), where

$$I_n = \int \varphi_n^*(\mu)\, H^{\mu}\, \varphi_n(\mu)\, d\tau \tag{7}$$

is the core energy for molecular orbital φ_n equal to the corresponding eigenenergy for the unperturbed problem,

$$J_{nm} = \int \varphi_n^*(\mu)\, \varphi_m^*(\nu)\, \frac{e^2}{r_{\mu\nu}}\, \varphi_n(\mu)\, \varphi_m(\nu)\, d\tau_{\mu}\, d\tau_{\nu} \tag{8}$$

being the Coulomb integral between the molecular orbitals φ_n and φ_m and

$$K_{nm} = \int \varphi_n^*(\mu)\, \varphi_m^*(\nu)\, \frac{e^2}{r_{\mu\nu}}\, \varphi_m(\mu)\, \varphi_n(\nu)\, d\tau_{\mu}\, d\tau_{\nu} \tag{9}$$

being the exchange integral between φ_n and φ_m, where $K'_{nm} = K_{nm}$ when φ_n and φ_m have the same spin function in Φ_A, and $K'_{nm} = 0$ when they have different spin functions in Φ_A.

Now, as the length of the cloud of the π electrons is large compared to its width, we may assume that approximately

$$r_{\mu\nu} = |x_\mu - x_\nu|. \tag{4a}$$

In view of the above considerations and the normalization of the φ term dependent on y and z we get from (7), (8), and (9)

$$I_n = \int \psi_n^* (x_\mu)\, H^\mu\, \psi_n (x_\mu)\, dx_\mu = E_n, \tag{7a}$$

where E_n is the eigenvalue corresponding to the Φ_n orbital,

$$J_{nm} = \int \psi_n^* (x_\mu)\, \psi_m^* (x_\nu)\, \frac{e^2}{|x_\mu - x_\nu|}\, \psi_n (x_\mu)\, \psi_m (x_\nu)\, dx_\mu\, dx_\nu \tag{8a}$$

and

$$K_{nm} = \int \psi_n^* (x_\mu)\, \psi_m^* (x_\nu)\, \frac{e^2}{|x_\mu - x_\nu|}\, \psi_m (x_\mu)\, \psi_n (x_\nu)\, dx_\mu\, dx_\nu. \tag{9a}$$

In the case of a non-branched bond path we have the following boundary conditions

$$\psi (x) = 0 \tag{10}$$

on both ends of the path.

From (10) and from the normalizing condition

$$\int_0^l \psi^2 (x)\, dx = 1 \tag{11}$$

we get the following set of eigenvalues and eigenfunctions of the unperturbed problem ($V(x) = 0$)

$$E = E_n = \frac{h^2 n^2}{8 m l^2} \tag{12}$$

$$\psi_n = \sqrt{\frac{2}{l}} \sin \frac{n\pi}{l} x \quad (n = 1; 2; \ldots) \tag{13}$$

We assume that the free electron path exceeds for a distance $C - C$ beyond the last carbon atom in the conjugated system. The formulation (10) — (13) was first given by Kuhn (1949).

Now we shall evaluate the Coulomb and exchange integrals. We shall begin with the K integral. For molecular orbitals we assume generally normalized and orthogonalized functions of the type

$$\psi_i = A_i \sin \alpha_i x \quad \text{where } 0 \leqslant x \leqslant l \tag{14}$$

We must first find the most convenient form for the expression $1/|x_\mu - x_\nu|$. We get namely[2]

[2] This transformation may be easily deduced by means of δ function theory. See e. g. Ivanienko and Sokolov, 1953.

$$\frac{1}{|x_\mu - x_\nu|} = \frac{1}{2\pi^2} \int_{-\infty}^{+\infty} \frac{e^{ik|x_\mu - x_\nu|}}{k^2 + r^2}\, dk \int_0^\infty r\, dr \int_0^{2\pi} d\Theta \tag{15}$$

Now we can evaluate our K_{ij} exchange integral by putting for the molecular orbitals of a free electron (14) into the expression for K_{ij}. Thus we have

$$K_{ij} = \int_0^l \int_0^l A_i \sin a_i x_\mu\, A_j \sin a_j x_\nu \frac{e^2}{|x_\mu - x_\nu|} A_j \sin a_j x_\mu\, A_i \sin a_i x_\nu\, dx_\mu\, dx_\nu$$

where x_μ and x_ν denote the coordinates of the first and second electron respectively. Integration is performed along the whole free electron path. Denoting $a_j + a_i$ by k_1, and $a_j - a_i$ by k_2 we get for the last formula the form

$$K_{ij} = \frac{1}{4} A_i^2 A_j^2 \int_0^l \int_0^l [\cos k_1 x_\mu \cos k_1 x_\nu - \cos k_2 x_\mu \cos k_1 x_\nu -$$

$$- \cos k_1 x_\mu \cos k_2 x_\nu + \cos k_2 x_\mu \cos k_2 x_\nu] \cdot \frac{e^2}{|x_\mu - x_\nu|}\, dx_\mu\, dx_\nu \tag{16}$$

Each component of this integral may be calculated separately. We shall consider first the integral

$$C = \int_0^l \int_0^l \cos k_1 x_\mu \cos k_2 x_\nu \cdot \frac{e^2}{|x_\mu - x_\nu|}\, dx_\mu\, dx_\nu, \tag{17}$$

which by formula (15) becomes

$$C = \frac{e^2}{\pi} \int_0^l \int_0^l \cos a x_\mu \cos c x_\nu \int_{-\infty 0}^{+\infty \infty} \frac{e^{ik|x_\mu - x_\nu|}}{k^2 + r^2}\, dk\, r\, dr\, dx_\mu\, dx_\nu$$

For clarity we have replaced k_1 by a, and k_2 by c. After performing the succesive integrations, we obtain the following expression

$$\frac{\pi}{e^2} \cdot C = \frac{\pi^2}{c + a} \cos^2 \frac{c + a}{2} l + \pi [\cos cl + \cos al] \left\{ \frac{c\, si(lc) \cos lc - a\, si(la) \cos la}{c^2 - a^2} \right\} \tag{18}$$

In the course of integration we have taken into account the boundary conditions for the free electron model (10). It may easily be seen that the result is symmetrical in relation to c and a.

To calculate the exchange integral K, we must also find the value of $(\pi/e^2)C$ when $c = a$. This value will be equal to the limit of the last expression when $c \to a$.

$$\int_{\infty -\infty 0}^{\infty +\infty l} \int_0^l \frac{1}{k^2 + r^2} e^{ik|x_\mu - x_\nu|} \cos a x_\mu \cos a x_\nu\, r\, dr\, dk\, dx_\mu\, dx_\nu$$

$$= \frac{\pi^2}{2a} \cos^2 al + 2\pi \cos al\, [t\, si(lt) \cos lt]'_{t=a} \cdot \frac{1}{2a} = \frac{\pi}{a} \cos^2 al \cdot Si(la) \tag{19}$$

Evaluating the derivative, we have also considered the boundary conditions for our problem. We get obviously a similar expression when we have c instead of a.

Taking advantage of the above results the Coulomb integral J for our problem will easily be evaluated. In our case it has the form

$$J_{ij} = \int_0^l \int_0^l A_i \sin a_i x_\mu \, A_j \sin a_j x_\nu \cdot \frac{e^2}{|x_\mu - x_\nu|} A_i \sin a_i x_\mu \, A_j \sin a_j x_\nu \, dx_\mu \, dx_\nu$$

$$= \frac{1}{4} A_i^2 A_j^2 \int_0^l \int_0^l (1 - \cos 2a_i x_\mu - \cos 2a_j x_\nu + \cos 2a_i x_\mu \cdot \cos 2a_j x_\nu) \, dx_\mu \, dx_\nu \qquad (20)$$

The last integral is quite similar to that evaluated in (18); the second and third ones readily follow from it. The first element in J_{ij}, i. e. the integral

$$\int_{-\infty}^{\infty+\infty} \int_0^l \int_0^l \frac{e^{ik|x_\mu - x_\nu|}}{k^2 + r^2} r \, dr \, dk \, dx_\mu \, dx_\nu,$$

may be evaluated by finding the limit of the expression $\frac{\pi}{a} \cos^2 al \, Si(la)$ when $a \to 0$. The result is πl. The evaluation of the J_{ii} type integral presents no difficulty.

The final form of the integrals in the *AS FEMO* method for the non-branched model is

$$K_{ij} = A_i^2 A_j^2 \cdot \frac{e^2}{4} \left\{ \frac{\cos^2 k_1 l}{k_1} Si(lk_1) + \frac{\cos^2 k_2 l}{k_2} Si(lk_2) - \frac{2\pi}{k_1 + k_2} \cos^2 \frac{k_1 + k_2}{2} l \right.$$

$$\left. - 2 [\cos k_1 l + \cos k_2 l] \cdot \frac{k_1 \, si(lk_1) \cos lk_1 - k_2 \, si(lk_2) \cos lk_2}{k_1^2 - k_2^2} \right\} \qquad (21)$$

$$J_{ij} = A_i^2 A_j^2 \cdot \frac{e^2}{4} \left\{ l + \frac{\pi}{2k_1} \cos^2 k_1 l + \frac{1}{2} \cos k_1 l \cos k_2 l \times \right.$$

$$\times \frac{(k_1 + k_2) \, si(k_1 + k_2) \, l \cos (k_1 + k_2) \, l - (k_1 - k_2) \, si(k_1 - k_2) \, l \cos (k_1 - k_2) \, l}{k_1 \cdot k_2}$$

$$- \frac{\cos^2 (k_1 + k_2) \frac{l}{2}}{k_1 + k_2} [\pi + 2 \cos (k_1 + k_2) \, l \, si \, (k_1 + k_2) \, l]$$

$$\left. - \frac{\cos^2 (k_1 - k_2) \frac{l}{2}}{k_1 - k_2} [\pi + 2 \cos (k_1 - k_2) \, l \, \mathrm{si} \, (k_1 - k_2) \, l] \right\} \qquad (22)$$

$$J_{ii} = A_i^4 \cdot \frac{e^2}{4} \left\{ l + \frac{\cos^2 (2a_i l)}{2a_i} \cdot Si \, (2a_i l) - \frac{\cos^2 a_i l}{a_i} [\pi + 2 \cos 2a_i \, l \, si \, (2a_i \, l)] \right\} \qquad (23)$$

k_1 and k_2 have the same meaning as previously described; a_i is the coefficient at x for a given molecular orbital.

Finally we must consider the electronic configurational interaction problem in *AS*

FEMO method. The singular Φ_A wave function may be, or may not be, a good approximation to the complete π-electronic wave function Ω_S of the given state of the electron system in the molecule. When this function suffices, the energy may be computed directly from *Eg.* (6), but when several Ω_S have to be taken into account, we must include the configurational interaction by applying the variational calculus to a linear combinations of Φ_A functions.

The Ω_S eigenfunction of the state may be written in the form

$$\Omega_S = \sum \lambda_i \Phi_i, \tag{24}$$

where Φ_i denote AS FEMO wave functions for a given type of symmetry, e. g. successively with the increase in energy. The energies E_i correspond to Φ_i. Now if we introduce the interaction between the configurational states and if we have as many AS FEMO wave functions as possible, then the best energies and wave functions will result, this being consistent with the primary application of the free electron molecular orbitals.

Thus, in order to obtain the eigenvalues for the energy E and the corresponding eigenfunctions, we must solve the secular equation

$$\begin{vmatrix} E_{\mathrm{I}} - E & (\Phi_{\mathrm{I}} \mid \Phi_{\mathrm{II}}) & (\Phi_{\mathrm{I}} \mid \Phi_{\mathrm{II}}) \dots \\ (\Phi_{\mathrm{II}} \mid \Phi_{\mathrm{I}}) & E_{\mathrm{II}} - E & \dots \\ \dots & \dots & \dots \end{vmatrix} = 0, \tag{25}$$

where

$$(\Phi_{\mathrm{I}} \mid \Phi_{\mathrm{II}}) = \iint \Phi_{\mathrm{I}}^{*} \sum_{\mu<\nu} \frac{e^2}{r_{\mu\nu}} \Phi_{\mathrm{II}} \, d\tau_\mu \, d\tau_\nu.$$

The entire method is strictly parallel to that given by Craig (1950) for antisymmetrized molecular orbitals LCAO.

Now we ought to evaluate the non-diagonal matrix elements of our secular equation. They are built of integrals over molecular orbitals of the type

$$[ij \mid kl] = \iint \varphi_i^{*}(\mu) \, \varphi_j(\mu) \frac{e^2}{r_{\mu\nu}} \varphi_k^{*}(\nu) \, \varphi_l(\nu) \, d\tau_\mu d\tau_\nu \tag{26}$$

For the non-brached free electron model, we get for this integral the particular form

$$A_i \, A_j \, A_k \, A_l \iint \sin \alpha_i \, x_\mu \sin \alpha_j \, x_\mu \frac{e^2}{| \, x_\mu - x_\nu \, |} \sin \alpha_k \, x_\nu \, \sin \alpha_l \, x_\nu \, dx_\mu \, dx_\nu.$$

From the above it may readily be seen that this integral may be expressed in terms of the integrals computed previously. These integrals will be of the C type.

2. Two simple examples: ethylene and butadiene

Though the AS FEMO method may be easily applied to much larger molecules, the ethylene and butadiene molecules have been chosen as examples not so much with regard to their simplicity as to the highly developed experimental investigation of their spectra and precise calculations by the LCAO method.

The entire method developed above has been applied to both ethylene and butadiene. The results have been compared then with those obtained by the far more complicated non-empirical method of antisymmetrized combination Slater $2p\pi$ atomic orbital products and experimental data. In the computations only the free electron molecular orbitals corresponding to the LCAO MO have been considered.

For ethylene we take two free electron molecular orbitals of the form

$$\psi_1 = \sqrt{\frac{2}{l}} \sin \frac{\pi}{l} x$$
$$\psi_2 = \sqrt{\frac{2}{l}} \sin \frac{2\pi}{l} x \tag{27}$$

Hence we get the energies of the configurational states (Parr and Crawford 1948).

$$\begin{aligned} 1 &= 2I_1 + J_{11} \\ 2 &= 2I_2 + J_{22} \\ \left.\begin{matrix} V_{12} \\ T_{12} \end{matrix}\right\} &= I_1 + I_2 + J_{12} \pm K_{12} \end{aligned} \tag{28}$$

$(1 \mid 2) = K_{12}$ is the nondiagonal element in the configurational interaction matrix, I_1 and I_2 are taken from (12), and J_{11}, J_{22}, J_{12}, K_{12} from (21)–(23).

The numerical values are given in tables I–III. The 1 and 2 states have the conventional meaning: we assign two electrons to ψ_1 and ψ_2 orbitals respectively. T is the triplet and V the singlet state which are obtained when there is one electron on each ψ_1 and ψ_2. N and Z states are obtained when the interaction between 1 and 2 states is taken into account.

Table I. The electronic interaction integrals for ethylene (in eV)

$J_{11} = 1{,}14779$	$J_{12} = 1{,}69665$
$J_{22} = 2{,}28848$	$K_{12} = 0{,}93242$

Table II. The electronic energy levels for ethylene (in eV) (without configurational interaction)

State	exact LCAO MO method[3] (Parr and Crawford 1948)	FEMO method
1 ($^1A_{1g}$)	0	0
2 ($^1A_{1g}$)	12,5	14,90
T ($^3B_{1u}$)	1,8	6,40
V ($^1B_{1u}$)	10,2	8,26
N ($^1A_{1g}$)	—1,3	—0,058

The interaction of 1 and 2 states in ethylene gives a decrease of the ground state only by about 0,06 eV, while the configurational interaction of the exact LCAO method gives for a similar decresae 1,3 eV.

[3] The yalues are calculated from Slater atomic orbitals with the effective charge — 3,18.

Table III. The electronic energy levels for ethylene (in eV) (configurational interaction included)

State	exact LCAO MO method[4] (Parr & Crawford 1948)	FEMO meth.	Experiment
N	0	0	0
T	3,1	6,46	3,1—5,6[4]
V	11,5	8,32	7,6
Z	15,0	15,02	...

The length of the free electron path in ethylene is taken to be equal to the 3-fold double bond length of this molecule, i. e. $l = 4{,}05\ \mathring{A}$.

For butadiene we take 4 free electron molecular orbitals (with successively increasing energies)

$$\psi_n = \sqrt{\frac{2}{l}} \sin \frac{n\pi}{l} x \quad (n = 1...4) \tag{29}$$

The lowest singlet configurational state at the energy E_0 with wave function V_0 has two electrons assigned to both ψ_1 and ψ_2. Excited configurational states arise when the electron is raised from ψ_i to ψ_j. We shall denote such states by V_{ij} and T_{ij} corresponding to singlet and triplet states respectively. We shall restrict ourselves to one-electron excited states. On the basis of (6) we get the following expressions for the energy differences

$$\begin{aligned}
E\begin{Bmatrix} V_{23} \\ T_{23} \end{Bmatrix} - E_0 &= I_3 - I_2 - J_{22} - 2J_{12} + 2J_{13} + J_{23} + K_{12} - K_{13} \pm K_{23} \\
E\begin{Bmatrix} V_{14} \\ T_{14} \end{Bmatrix} - E_0 &= I_4 - I_1 - J_{11} - 2J_{12} + 2J_{24} + J_{14} + K_{12} - K_{24} \pm K_{14} \\
E\begin{Bmatrix} V_{24} \\ T_{24} \end{Bmatrix} - E_0 &= I_4 - I_2 - J_{22} - 2J_{12} + 2J_{14} + J_{24} + K_{12} - K_{14} \pm K_{24} \\
E\begin{Bmatrix} V_{13} \\ T_{13} \end{Bmatrix} - E_0 &= I_3 - I_1 - J_{11} - 2J_{12} + 2J_{23} + J_{13} + K_{12} - K_{23} \pm K_{13}
\end{aligned} \tag{30}$$

where the plus and minus signs correspond to singlet and triplet states respectively.

The energies obtained for the states corresponding to different assignment of electrons to particular molecular orbitals may now be corrected by taking into account configurational interaction. As we are interested here in the lower excited states, only the lowest configurations of a given symmetry have been considered. It seems that by including a large number of configurations we would get only a small correction of our results (see the discussion below).

So we take for „mixing" V_0, V_{24} and V_{13} wave functions, all three of ^1A symmetry,

[4] The location of the lowest triplet state in ethylene is not quite clear yet; its symmetry is also not very certain. The strong absorption in ethylene at 7,68 eV and the symmetry of this state is undeniable. The investigations in the liquid nitrogen temperature (see Moser 1953) show the appearance of the triplet state at a relatively small distance from the singlet state — about 1,00 — 1,25 eV (Potts).

V_{23} and V_{14} of ^1B symmetry, T_{23} and T_{14} of ^3B symmetry, and T_{13} and T_{24} of ^3A symmetry[5].

Table IV. The electronic interaction integrals for butadiene (eV)

$J_{11} = 0{,}66408$	$J_{12} = 0{,}98163$	$J_{23} = 1{,}44256$	$J_{24} = 1{,}48901$
$J_{22} = 1{,}32405$	$J_{14} = 1{,}08311$	$J_{13} = 1{,}05366$	
$K_{12} = 0{,}53947$	$K_{23} = 0{,}73701$	$K_{14} = 0{,}064591$	
$K_{13} = 0{,}024884$	$K_{24} = 0{,}11659$		
$[11 \mid 13] = 0{,}31755$	$[11 \mid 24] = 0{,}38957$	$[13 \mid 24] = 0{,}07136$	
$[22 \mid 24] = 0{,}46093$	$[12 \mid 23] = 0{,}60594$	$[23 \mid 14] = 0{,}13106$	
$[22 \mid 13] = 0{,}34244$	$[12 \mid 14] = 0{,}06647$	$[12 \mid 34] = 0{,}64098$	

The approximate values for the matrix elements of configurational interaction (in eV)

$(V_0 \mid V_{13}) = 0{,}57$	$(V_{13} \mid V_{24}) = -0{,}50$	$(T_{13} \mid T_{24}) = -0{,}64$
$(V_0 \mid V_{24}) = 1{,}66$	$(V_{23} \mid V_{14}) = -0{,}38$	$(T_{23} \mid T_{14}) = -0{,}64$

Table V. The electronic energy levels for butadiene (eV) (without configurational interaction)

Configurational state	exact LCAO MO method (Coulson and Jacobs 1951)	FEMO method
^1A_g (V_0)	0	0
^1B_u (V_{23})	5,83	5,35
^1A_g (V_{13})	8,16	7,28
^1A_g (V_{24})	6,15	10,17
^1B_u (V_{14})	11,51	13,44
^3B_u (T_{23})	—0,78	3,88
^3A_g (T_{13})	2,76	7,23
^3A_g (T_{24})	4,66	9,94
^3B_u (T_{14})	7,26	13,31
N	—2,79	—0,32

Table VI. The electronic energy levels for butadiene (in eV) (configurational interaction included)

State	exact LCAO MO method (Coulson and Jacobs 1951)	FEMO meth.	Experim.
^1A_g	0	0	0
^1B_u	7,21	5,62	6,0
^1A_g	10,78	7,60	7,2
^1A_g	3,60	10,80	...
^1B_u	12,08	13,81	...
^3B_u	1,05	4,16	...
^3A_g	3,15	7,41	...
^3A_g	8,27	10,40	...
^3B_u	8,87	13,67	...

[5] The same system of electronic configurations in butadiene was considered by Pariser & Parr (1953) in their semi-empirical method. The experimental results for both molecules are taken from this paper.

The numerical results for configurational interaction matrix elements as well as electronic repulsion integrals and energies of the states are given in the tables below. By solving four secular equations corresponding to the four types of symmetry, we get the final results for energies of the electronic states which are given in table VI.

The length of a free electron path in butadiene was taken to be equal to the five-fold mean length of the bond in the conjugated molecules, i. e. 7,0 Å. Substituting the parameters of the molecular (14) — type orbitals, it may be shown that for these orbitals all the values connected with the electronic interaction in the corresponding molecules (exchange integrals, Coulomb integrals and configurational interaction matrix elements) are inversely proportional to the length of the free electron path[6].

By the method given above any molecules having nonbranched free electron bond paths may be calculated[7]. No other assumption concerning the empirical quantities than the length of the bond need to be introduced. A generalization of the theory for any unsaturated hydrocarbons with conjugated systems of double bonds will be presented later.

3. Discussion

The first and the most important drawback of the only purely theoretical method, developed so far for investigating the spectra of unsaturated conjugated hydrocarbons, is the disagreement of the results with experiment. Few molecules have been examined so far by this method and the results have been compared with the experimental data which are far from being complete. Full computations have been made only for ethylene, butadiene, benzene. In spite of their incompleteness the present experimental data point to serious drawbacks in the LCAO method.

In the present work which was concerned with the molecules containing unbranched chains of conjugated bond systems we discuss only the structure of the absorption spectra for ethylene and butadiene, where a more exact comparison of the given data with LCAO method and experiment is possible.

The energy levels for ethylene theoretically found by the LCAO method are qualitatively in agreement with experiment but quantitatively they are far from that. By AS FEMO method the error in estimation of the first singlet excited level for ethylene is reduced from 3,9 eV to about 0,7 eV.

---

[6] The free electron model of butadiene corresponds rather to the trans form of the molecule. The cis form could be considered as characterized by a somewhat shorter free electron path. Then the energy of the ground state and the energies of the excited states of the trans form would be lower than the corresponding cis energies, since the "core" part in the expressions for the energies and the part of the electronic interaction are positive and increase with decreasing l.

[7] The free-electron treatment of polyens (with $V = 0$ assumption) is not quite permissible. But for the case of the short chain the spectrum is not greatly effected by the localization of the π-electrons on the double bonds and this effect may be neglected.

It is well known that for butadiene, although the interaction between a large number of configurations is included in the calculations with LCAO method (Coulson and Jacobs 1951), even a qualitatively correct scheme cannot be obtained. The lowest excited singlet state is there a ^1A state obtained from the „perturbed" electron jump from level 2 to 4. V_{13} and V_{24}, when the configurational interaction is included, give states, the difference between them being as high as 7 eV. The results of the calculations by the self-consistent method, (Parr and Mulliken 1950) taking into account to a great extent the effect of configurational interaction, give at the same time the reverse succesion of these states. Furthermore, the lowest singlet excited state is in butadiene that of ^1B symmetry lying on the LCAO scheme just over 3,5 eV above the first excited ^1A state.

With such an unintelligible description of the positions of the energy states, a good quantitative agreement cannot be expected. The first excited state observed lies 1,2 eV lower than the lowest ^1B level of the LCAO method. For the second state in this method a corresponding term can hardly be found.

Now the present method gives for butadiene a reasonable succession of states in agreement with the results of the semi-empirical Pariser and Parr theory (1953) and with the calculations performed by means of a self-consistent field method by Parr and Mulliken (1950).

As far as the agreement with experiment is concerned, it seems to be even better than that for ethylene. The difference between the results of observations and those obtained from computations is about 0,4 eV, with only a small number of configurations included in the calculations.

The separation between the singlet and triplet level present another problem. In the LCAO method they are far too large. This shows this method to be unreliable in evaluating the exchange integrals. The real singlet-triplet separation for the lowest excited states is probably approximately eqnal to 1 eV (Parr and Mulliken 1950). This result is in no great discrepancy with the present method.

The characteristic feature of the method is that it gives relatively small values for the electronic repulsion molecular integrals. Thus the corresponding matrix elements, when the configurational interaction is taken into account, have smaller values than those built from molecular orbitals, which are the combinations of atomic $2p$ orbitals. This results in a descrease in the electron configuration interaction effect on the value of the energies of the states. At the same time the configurational interaction method has here a more perturbational character than for LCAO orbitals. The decrease of the ground state caused by the configurational interaction for the calculated molecules is many times less than that evaluated by the LCAO method. This fact allows at once for some insight into the system of energy states of the spectrum. The probability of mixing the states given by the theory is strongly reduced. Thus the necessity of applying a complicated mathematical formalism connected with the interaction of many configurations is also decreased.

From the above considerations it may be supposed that in our examples the

LCAO method based on the calculations of $2p$ atomic orbitals is not so well confirmed by experiment as the FEMO method delocalizing completely the π electrons along the free bond path of the molecules.

The second serious obstacle in applying the purely theoretical LCAO method lies in its computational difficulties. The present method avoids this difficulty to a great extent. All the integrals are computed in the molecular orbitals. Thus the necessity of expanding into integrals over atomic orbitals is avoided. There are no multicentered integrals, and for the integrals applied in the present method simple general formulae can be obtained.

The author wishes to express his deep gratitude to Dr W. Kołos for assistance in preparing the manuscript and many stimulating discussions.

КРАТКОЕ СОДЕРЖАНИЕ

Ольшевский. ЭЛЕКТРОННОЕ ВОЗДЕЙСТИЕ В МОДЕЛИ СВОБОДНОГО ЭЛЕКТРОНА ДЛЯ НЕРАЗВЕТВЛЕННЫХ СОПРЯЖЕННЫХ СИСТЕМ.

Представлен метод ASMO CI для молекулярных орбит свободного электрона в случае молекул о неразветвлённой системе сопряженных связи, при полной аналогии с теорией ASMO CI, развитой Гоепперт-Майер и Скляром и Крейгом для молекулярных орбит, как комбинацией линейных атомных орбит 2p.

Эта схема была применена к вычислению энергетических уровней в двух случаях: этилена и бутадиена. Полученные результаты сходятся с экспериментальными данными более, нежели результаты, полученные при помощи аналогичных вычислений методом LCAO MO. Происходит это в особенности при сепарации синглетно-триплетной первых возбуждённых состояний. Кроме того получено значительное уменьшение эффекта конфигурационного воздействия в сравнении с методом LCAO MO.

REFERENCES

Coulson, C. A. and Jacobs. J., *Proc. Roy. Soc.*, **206**, 287 (1951).
Craig, D. P., *Proc. Roy. Soc.*, **200**, 474 (1950).
Goeppert-Mayer, M. and Sklar, L. A., *J. chem. Phys.*, **6**, 645 (1938)
Ivanenko and Sokolov, *Klasicheskaya Teorija Pola*, Moskva, 1952.
Kuhn, H., *Helv. chim. Acta*, **32**, 2247 (1949).
Moser, C. M., *Trans. Faraday Soc.*, **49**, 1239 (1953).
Mulliken, R. S., *J. Chim. phys.*, **46**, 497 (1949).
Pariser, R. and Parr, R. G., *J. chem. Phys.*, **21**, 767 (1953).
Parr, R. G. and Crawford, B. L., *J. chem. Phys.*, **16**, 526 (1948).
Parr, R. G. and Mulliken, R. S., *J. chem. Phys.*, **18**, 1338 (1950).
Pullman, B. and Pullman, A., *Les théories électroniques dans la chimie organique*, Paris, 1952, (with detailed references on the LCAO MO method).
Ruedenberg K. and Scherr, C. W., *J. chem. Phys.*, **21**, 1565 (1953), (with detailed references on the FEMO method).
Ruedenberg K., *J. chem. Phys.*, **22**, 1878 (1954).

ERRATA

Acta Physica Polonica, **14**, 407 (1955):

ANGULAR DISTRIBUTION OF DEUTERONS FROM ^{9}Be (p,d)^{8} Be

By J. Dąbrowski and J. Sawicki

Institute of Physics, Polish Academy of Science, Warsaw

The angular distributions of deuterons from the ^{9}Be(p,d) ^{8}Be reactions and tritons from the ^{9}Be(d,t)^{8}Be reaction were analyzed in our previous papers (1954, 1955a, 1955b, 1956). The results of these papers require a correction. Namely, the expression for $I_r(k)$ adopted from the paper by H. Überall contains an error overlooked in our previous papers. In Eq. (I, 3b), in the denominator of the expression for N^2, n_0 should be replaced by n_0^2, and the opposite sign should be adopted for N_a. The sign of the term $k \sin kr_0$ $(1 + 1/\alpha r_0)$ in Eq. (I. 9b) should be changed to positive.

The most important correction concerns the absolute values of the cross sections. Table I of paper (II) and Table II of the Supplement (1956) should read:

TABLE I

r_0 in 10^{-13} cm	$E_p = 6.5$ MeV		$E_p = 22$ MeV	
3	0.13	0.10	0.20	0.13
5	0.29	0.16	0.36	0.09*
7	0.51*	0.16*	0.42*	0.02*
	Born	Butler	Born	Butler

TABLE II

θ_s	Theoretical values for $r_0 = 5 \times 10^{13}$ cm	
	Born	Butler
0°	303	106
8°	274	87
12°	242	67

For $E_p = 5$—8 Me V and $\theta_L = 20°$ for $r_0 = 5 \times 10^{-13}$ cm (Born) one gets $d\sigma_L/d\Omega_L =$ $= 0.22$ barn/ster, i. e., a value about 9 times too great — instead of 0.26 barn/ster, i. e., a value about 11 times too great.

For the ^{9}Be(d,t) ^{8}Be reaction $(d\sigma_S/d\Omega_S)_{\Theta_S=0°} = 34$ mb/ster and 39 mb/ster instead of 87.12 and 72.30 mb/ster for $r_0 = 5 \times 10^{-13}$ cm and $r_0 = 7 \times 10^{-13}$ cm respectively. The respective total cross sections are 44 mb and 27 mb (instead of 110.9 mb and 50.6 bm). The angular distribution for this reaction remains unchanged.

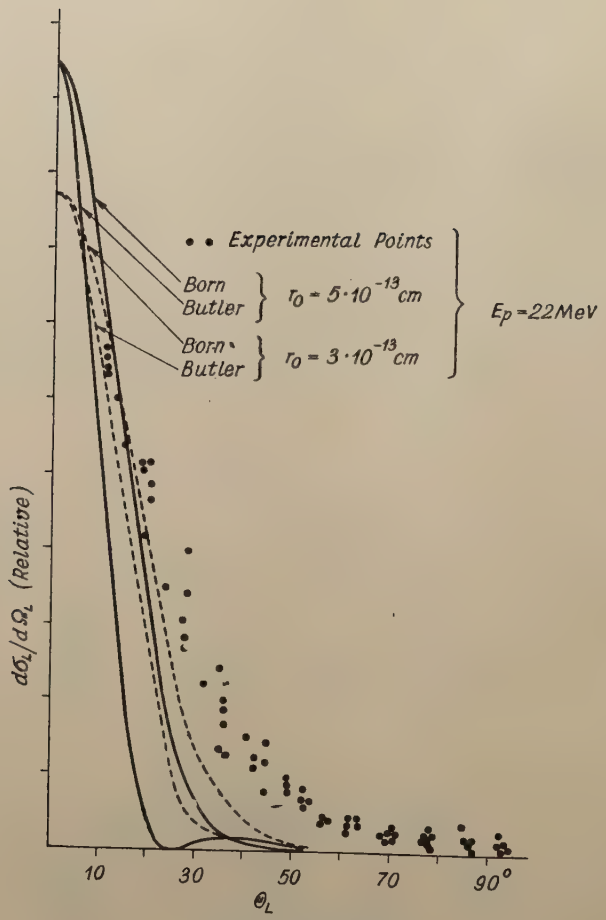

Fig. 2 (corrected)

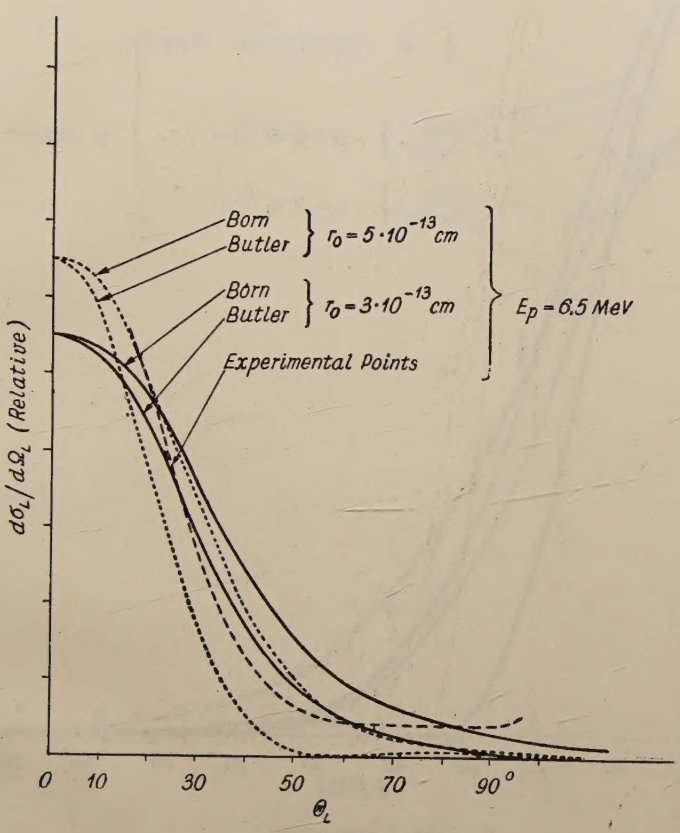

Fig. 3 (corrected)

The agreement of the calculated angular distributions with the experimental data for the (p, d) reaction is only very slightly changed (see the corrected Figs 2, 3, 5). The only difference is that the best value of r_0 should be somewhat smaller than 5×10^{-13} cm. The curves for $r_0 = 7 \times 10^{-13}$ cm are omittedi n the corrected figures since they are in distinct daisgreement with experiment.

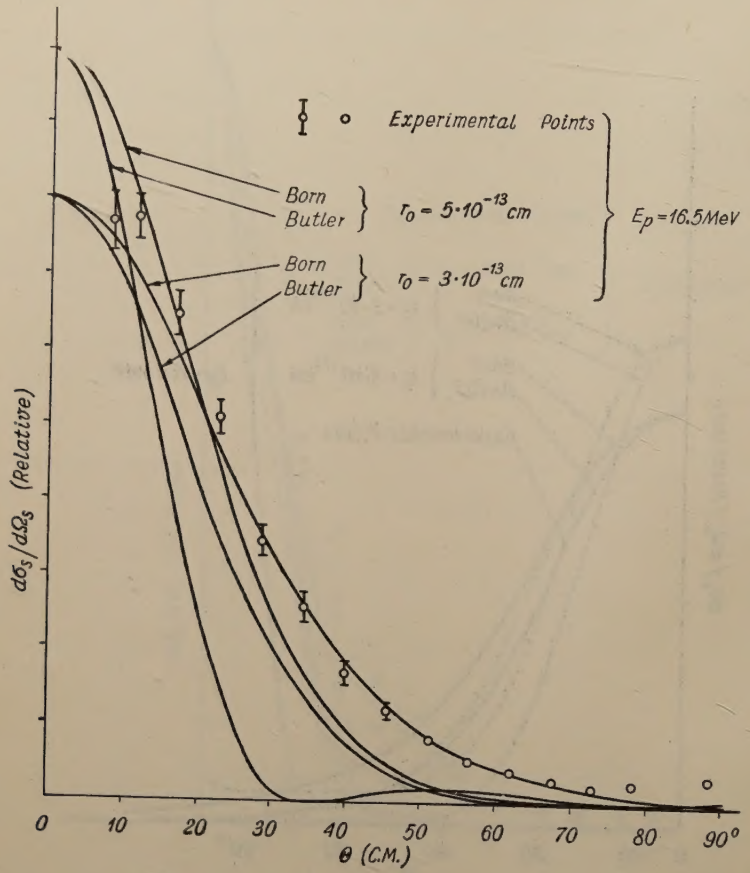

Fig. 5 (corrected)

REFERENCES

Dąbrowski, J. and Sawicki, J., *Nuovo Cimento*, **12**, 293 (1954); *Acta phys. Polon.* **14**, 143 (1955a); **14**, 407 (1955 b); **15**, 3 (1956).

Überall, H., *Z. Naturforsch.*, **8a**, 142 (1953).

Volumen XIV (1955) — Fasciculus 5